



**HAL**  
open science

# Hydrological & geomorphological analysis of the Upper Trusan River to assess remediation for riverbank integrity. WWF-Malaysia Project Report

Baptiste Marteau, Chris Gibbins, Ramon J. Batalla, Damià Vericat

## ► To cite this version:

Baptiste Marteau, Chris Gibbins, Ramon J. Batalla, Damià Vericat. Hydrological & geomorphological analysis of the Upper Trusan River to assess remediation for riverbank integrity. WWF-Malaysia Project Report. WWF Malaisie. 2018. hal-04648824

**HAL Id: hal-04648824**

**<https://hal.science/hal-04648824>**

Submitted on 15 Jul 2024

**HAL** is a multi-disciplinary open access archive for the deposit and dissemination of scientific research documents, whether they are published or not. The documents may come from teaching and research institutions in France or abroad, or from public or private research centers.

L'archive ouverte pluridisciplinaire **HAL**, est destinée au dépôt et à la diffusion de documents scientifiques de niveau recherche, publiés ou non, émanant des établissements d'enseignement et de recherche français ou étrangers, des laboratoires publics ou privés.



**Hydrological &  
geomorphological analysis of  
the Upper Trusan River to assess  
remediation for riverbank  
integrity**

**WWF-Malaysia Project Report**



August 2018

# **Hydrological & Geomorphological analysis of the Upper Trusan River to assess remediation for riverbank integrity**

By

Dr. Baptiste Marteau

Prof. Chris Gibbins

Dr. Ramon Batalla

Dr. Damià Vericat

Report Produced Under Project SW010603-831-CORP SCP-CIMB

Long Semadoh Riverbank Instability and Erosion Project

August 2018

## Executive summary

1. This report was commissioned by WWF Malaysia in response to concerns expressed by local communities in the Long Semadoh area. Changes in the behaviour of the Trusan river threaten their livelihoods by eroding banks and depositing fine sediment on their rice paddies. The village people have started to tackle these issues by channelizing sections of the river and reinforcing banks with large boulders. However, these represent only localised, temporary measures that in some instances may actually further increase the risks of bank erosion; moreover, they do not address the cause of the problem so cannot be considered to be long-term solutions.
2. The overall goal of the work summarised in this report was to assess the extent and severity of erosion in the river and understand the causal processes. The work focussed on a 5.2 km-long section of the Upper Trusan, with the objective of understanding fluvial processes at the catchment, river corridor and channel scales in order to identify the causes of what villagers consider as “river erosion problems”. Based on this understanding we propose a series of recommendations to help address the root causes of the problems, as well as suggesting shorter-term remedial actions to help address some of the most acute problems. Recommendations are based on a review of best practice undertaken in parallel with the current study (Marteau *et al.*, 2018).
3. The combination of walkover field surveys, field observations, ground- and aerial images obtained by an Unmanned Aerial Vehicle (UAV, or drone) allowed maps of the spatial distribution and severity of bank erosion to be produced. This information was combined with analyses using a 2-dimensional hydraulic model to identify erosion ‘hot-spots’ and understand the reasons for these.
4. The paucity of available long-term discharge data made it impossible to properly assess changes in the hydrology of the study section. However, analysis of rainfall data collected over 50 years at Long Semadoh indicates that precipitation has not changed significantly in the area. The Upper Trusan catchment has suffered only limited deforestation, with most land clearance concentrated within one sub-catchment over the last 3-4 years. Increased soil erosion and runoff is expected in cleared areas. The deforestation recorded in this sub-catchment can be directly linked to the complaints of the villagers from Punan Trusan, where rice paddies are periodically covered by fine sediment after floods.
5. A total of 30% of the riverbank length in the Upper Trusan suffers from high to severe erosion, of which approximately 50% is due to the undermining of banks (i.e. collapse of the top of the banks once loose material underneath is flushed because of high shear stresses near the bed). Analysis of riparian cover showed that erosion is greatest

in areas where riparian trees have been removed. In some places erosion is linked to human intervention within the active channel (e.g. channel engineering) and trampling by cattle. In some locations bank retreat of 18 m is evident over the last three years. These causes can be addressed quite easily by thoughtful management of bankside and riparian areas. In other places major landslides have been caused by forest clearance on steep slopes directly adjacent to the river, and these are delivering large volumes of fine sediment to the channel.

6. Hydraulic models indicated that in some areas erosion can be explained by high shear stresses at bankfull discharge. However, models also indicated that severe erosion is occurring in some locations where shear stresses remain only moderate at bankfull discharge. These locations are where riparian trees have been cleared completely.
7. We recommend a series of actions to improve management at the catchment, river corridor and local (river reach) scales. Catchment actions include strategies to limit forest clearance, especially close to the channel on steep slopes, limiting construction of new tracks and better management of existing ones. At the river corridor scale, we suggest that because the Trusan is a high energy system some areas should be 'given back to the river' and left to erode. To counter this, we recommend some other corridor scale actions to safeguard other locations – namely, a presumption against any further clearance of riparian vegetation and better management of cattle, including controlling their movement and erecting fences to keep them away from the riverbank. At the local scale, we propose some intervention to deal with the most severe cases of erosion. The local interventions all involve bio-engineering approaches, using various plants and organic materials to help stabilize sections of bank.
8. Although based on detailed analysis of fluvial dynamics within the Trusan, our recommendations require discussion amongst stakeholders before any actions are taken. In particular, our recommendations need to be matched against local priorities and perceptions of the magnitude and causes of the problems. Most specifically, where we suggest local interventions, these need to be costed and assessed for feasibility, so technical specialists (engineers) need to be included in discussions once consensus has been reached about priorities and key sensitive locations.
9. In keeping with best practice, we strongly recommend that a program of ongoing survey and monitoring is implemented. This should include periodic repeats of the hydrologic and geomorphic assessments presented in this report, as well as installation of some monitoring equipment to continuously record discharge and suspended sediment in the reach. The overall goal of the survey and monitoring would be to assess the success of actions taken to address the flooding and erosion issues experienced in the Upper Trusan.



**University of  
Nottingham**  
UK | CHINA | MALAYSIA



**CTFC**



## Contents

Executive summary .....	1
Contents.....	4
1 Introduction and scope.....	5
2 Methods.....	7
2.1 Overview of data and approach.....	7
2.2 Analysis of existing data .....	7
2.2.1 Hydrological and climatic data.....	7
2.2.2 Satellite images.....	9
2.3 New data collection .....	10
2.3.1 UAV flights and production of DEMs.....	10
2.3.2 Hydraulic cross-sections and models .....	13
2.3.3 Grain-size of bed surface sediments .....	14
2.3.4 Bed mobility - painted patches .....	16
2.3.5 Armouring: vertical variability of bed sediments.....	16
2.3.6 Field-based observations and assessment of bank erosion .....	17
3 Findings.....	18
3.1 Rainfall trends .....	18
3.2 Land cover and land use changes .....	21
3.2.1 Tracks and roads.....	21
3.2.2 Forest clearance and disturbance.....	22
3.3 Inventory of riverbank erosion within the Upper Trusan catchment.....	24
3.3.1 Severity of bank erosion.....	25
3.3.2 Influence of local controls on erosion .....	31
3.4 Bed sediment size .....	33
3.4.1 Bed mobility .....	36
3.4.2 Bed armouring .....	37
3.5 Hydraulic modelling .....	38
4 Conclusions from the assessment of factors influencing erosion .....	42
5 Recommendations .....	44
5.1 Catchment scale.....	44
5.2 River corridor scale .....	47
5.3 Localised interventions.....	50
5.4 The need for ongoing hydrological monitoring and survey .....	54
6 Reference list.....	56
7 Appendices .....	57

## 1 Introduction and scope

The Trusan is a 2,515 km<sup>2</sup> catchment located in North-eastern Sarawak, Malaysia (Figure 1). The present study focused specifically on the Upper Trusan (catchment area 140 km<sup>2</sup>), in a section that has been experiencing erosion and flooding problems in recent years. This approximately 5.2 km-long section extends from the village of Punan Trusan downstream to Long Semadoh (Figure 1c).

The geographical area and scope of the project were set by WWF, based on concerns expressed about erosion and flooding in the area. Research objectives addressed by this report were set out in the Tender document prepared by WWF. These objectives are to:

1. Understand the hydrology and hydraulics of the Upper Trusan river and how these affect riverbank integrity
2. Provide recommendations for long-term remediation of existing riverbanks affected by erosion
3. Recommend interim actions that can be taken to secure the banks, while the long-term remediation actions are being implemented.

Based on these objectives, WWF also set out a number of more specific research questions:

- a) What are the main factors contributing to riverbank erosion?
- b) Where are the most vulnerable areas?
- c) What short-term remedial actions can be taken in these vulnerable areas to prevent further erosion?
- d) What longer-term preventative actions should be taken to minimize erosion in sections currently not affected?
- e) What monitoring actions should be carried out to measure the effectiveness of the restoration and prevention plan?

In addition, WWF specified the need to construct a hydraulic model to aid understanding of flow conditions and geomorphic integrity within the study section, and to help underpin recommendations. This report addresses the objectives and questions set out by WWF.

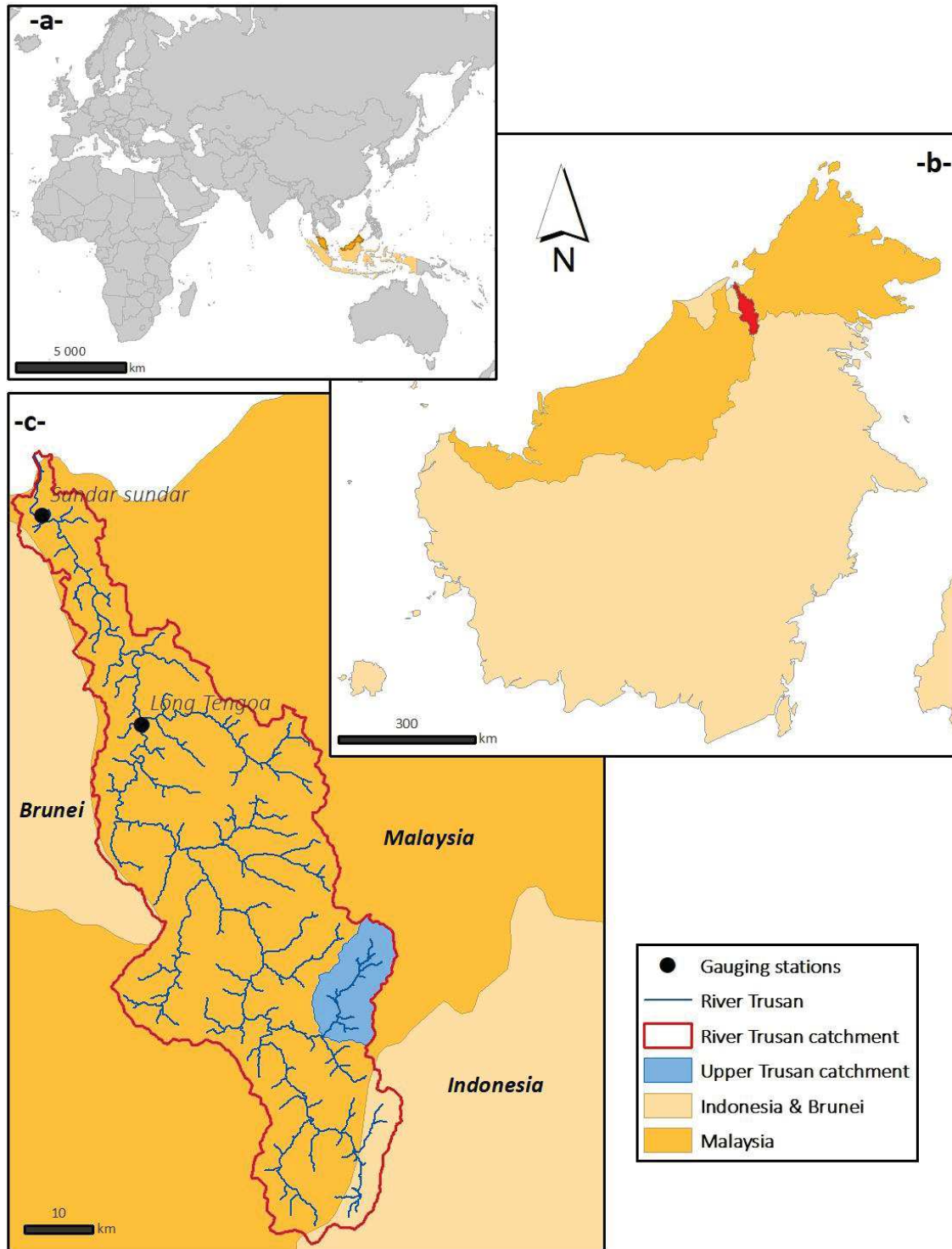


Figure 1. (a) Location of Malaysia, (b) location of the River Trusan catchment within the island of Borneo, and (c) location of the Upper Trusan catchment.

## 2 Methods

### 2.1 Overview of data and approach

The report is based on existing and new data sets. Existing data on river discharge and rainfall in the Trusan catchment were obtained from the Department of Irrigation and Drainage (DID), following requests submitted in December 2017. Existing Landsat satellite images were used to assess current landcover and historic landcover change. New data were collected during two field surveys, conducted from 2-9 February and 2-7 March 2018. The first of these campaigns included an initial walk-over survey of the whole 4.4 km section, in the company of WWF staff. Based on assessments from this walk-over, the section was extended slightly (total 5.2 km) and then divided into a number of shorter reaches; information on flow hydraulics, bed sediment grain-size distributions and armouring was collected from each reach, while patches of bed were painted (used as tracers) to help assess sediment movement. Aerial photographic surveys of the whole section were undertaken using an Unmanned Aerial Vehicle (UAV). These images were complemented with others taken during the walk-over survey. During the second campaign, painted patches were revisited to assess any bed mobility that might have occurred during the intervening period, and UAV flights were undertaken at a lower altitude than in the first campaign in order to build Digital Elevation Models (DEMs). Ground control points were surveyed using an rtk-GPS to help with construction of the DEMs developed from the aerial photos; these DEMs were used for visualisation (e.g. mapping erosion) and for hydraulic modelling. The following sections provide details of each of these aspects of the work.

### 2.2 Analysis of existing data

#### 2.2.1 Hydrological and climatic data

DID has a total of nine monitoring stations within the Trusan catchment. Two of these are combined rainfall and discharge gauging stations (Sundar Sundar and Long Tengoa), six of the remainder are rainfall-only stations, and one (a second station at Long Tengoa) monitors discharge. Data were requested for all stations within and downstream from the monitoring section; two (Rutoh and Ba'Kelalan) are upstream and in a different sub-catchment and so data were not requested for these. Data supplied by DID are summarised in Table 1.

The critical data needed for the current study are rainfall and discharge (Q) at Long Semadoh. Discharge is not gauged at Long Semadoh and the nearest downstream gauge (measuring water level/stage) is at Long Tengoa. This site is not ideal for understanding any changes that may be happening at Long Semadoh, as it is situated downstream from the confluence with the Sungai Kelalan, a major tributary. It would be inappropriate to assume that discharge at

Long Semadoh could be estimated simply as a scaled function of the decrease in catchment area from the Tengoa gauge as landcover in the Kelalan is different to the mainstem Trusan at Long Semadoh and so the two catchments most likely have different rainfall-runoff relations. Thus, rather than attempting to assess long term hydrological trends for Long Semadoh, we have simply looked for evidence of patterns at Long Tengoa. Even so, the Long Tengoa data are not ideal for this, as they are very patchy (i.e. many whole years and months are missing from the time-series; Figure 2) and the stage-discharge relationship supplied by DID covers a different period to the stage data (data series 1999-2010; stage-discharge relationship October 1983 to May 1985). Thus, due to uncertainties about the data (see additional comments in caption to Fig 2), assessments of hydrological change in the Trusan needed to be treated with care. Rather than discussing changes in discharge magnitude *per se*, we confine assessment to changes in the numbers of flood events occurring within specified time periods. For this we used the number of days that discharge exceeded 1.5 times the long-term average (i.e. average for the whole data period, excluding missing values). We considered these situations as flood events, a criterion widely used in the literature (e.g. García-Ruiz *et al.*, 2005).

As indicated by Table 1, rainfall data are available for a longer period and are more complete than the discharge data. These are used to assess whether there is any evidence of changes in rainfall in the Upper Trusan.

Table 1. Summary of data made available by DID.

Station name	Data	Time period(s)	Comments
Long Semadoh	Rainfall	1950-2017	Daily total (mm)
Sundar	Rainfall	1948-2017	Daily total (mm)
Long Tengoa	Rainfall	1981-2017	Daily total (mm)
Long Tengoa	Stage/level	1999-2010	Mean daily stage (m)
Ba' Kelalan	Rainfall	1980-2017	Daily total (mm)
Rutoh	Rainfall	1998-2017	Daily total (mm)
Long Merarap	Rainfall	1998-2017	Daily total (mm)
Trusan	Rainfall	1971-2017	Daily total (mm)

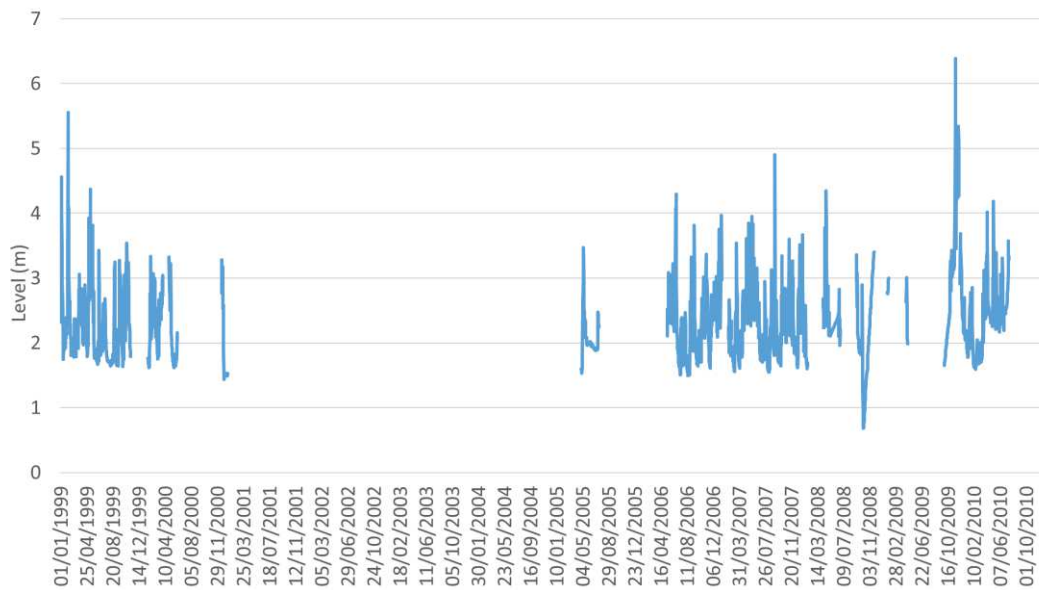


Figure 2. Water level (stage) data available for Long Tengoa, the nearest gauging station to the study section. Data supplied by DID. Water level is recorded at Long Tengoa, and this has been converted to discharge ( $Q$ ) using the rating curve supplied by DID. Note that the rating curve yielded around 10 daily values discharges above  $1500 \text{ m}^3 \text{ s}^{-1}$ , with some as high as 3000. These were removed from the data set.

### 2.2.2 Satellite images

Landsat satellite images, freely available (earthexplorer.usgs.gov), were used to assess landcover change. This analysis was primarily focussed on 3 elements: (i) to determine the length and timing of road construction in the catchment, (ii) to assess change in forest cover (deforestation and forest disturbance) and (iii) to monitor changes in the distribution and extent of rice paddies across the River Trusan's floodplain. To do so, 6 satellite images were used for years between 2007 and 2016 (Table 2). Almost all images had less than 6% of cloud cover within the area of interest; the exception was 2016, for which two images were needed because of high cloud density (final cloud cover <6%).

Table 2. Origin and date of collection of Landsat satellite images used in this study.

Mission	Date of collection	Resolution
Landsat 5	26/06/2007	30 m
Landsat 5	03/09/2009	30 m
Landsat 8	21/06/2011	30 m
Landsat 8	26/04/2014	30 m
Landsat 8	04/07/2016-10/01/2016	30 m

Roads and tracks were digitised manually for each year. The development of the track network was further explored using the Google Earth Engine (<https://earthengine.google.com/timelapse/>), specifically to develop a more accurate timeline of road and track construction, and to assess their development prior to 2007. Forest cover

change was assessed using CLASlite, a forest monitoring package developed with the aim of providing automated identification of deforestation and forest degradation from satellite imagery (Asner, 2009). The extent of rice paddies within the floodplain was assessed using the NDWI index (Gao, 1996), which is an index based on pixel colours (using the green and infra-red bands), is able to detect surface water and wetlands. Although it is not capable of distinguishing between river channels, ponds and paddies, based on the knowledge of the geometry and hydrology of the paddy areas developed during the field surveys, we are confident in the NDWI assessments.

## 2.3 New data collection

### 2.3.1 UAV flights and production of DEMs

UAV flights were undertaken using a Mavic Pro drone. This has a built-in 30 axis Gimbal so that the camera is stable and can be set to the required angle. The camera has a CMOS sensor with a 4000 x 3000-pixel (12.35 MegaPixel) maximum resolution for stills and a 4K (3840x2160 pixel) resolution for video. All images and resulting point clouds and DEMs presented in this report were captured directly as jpg stills (i.e. rather than extracting images from video footage), with the image resolution set at 12.35 MP. ISO was set to automatic, and so varied from 100-1600 depending on light conditions.

As far as possible flights were undertaken in slightly overcast conditions, to help avoid water glare, and in the middle period of the day so that the sun was overhead. However, due to hourly and day-to-day variation in cloud cover and the logistics of field surveys, this was not always possible. Nonetheless, to ensure similar conditions in images used for orthophotos, all images for a given reach were collected in a single run (lasting around 30 mins).

Flight paths all used a double zig-zag pattern, designed to optimize data collection for the production of 3D point clouds (topographic information) and DEMs. For this pattern, one path follows the up-to-downstream direction and then the other follows a zig-zag laterally across the channel. During the first field campaign, flights of the whole study section were made at an altitude of  $150\pm 7$  m (above ground level). The orthophotos produced from these flights were used primarily for visualization and mapping of erosion areas. The high altitude meant that much of the floodplain was captured in the images, permitting assessment of relations between activities in the immediate vicinity of a given reach (e.g. forest clearance) and riverbank erosion. On average, the photos cover the river course and approximately 200 meters of the floodplain. The whole 5.2 km reach was then subdivided into a series of shorter reaches, numbered sequentially from up- to down-stream. Three of these reaches (#1, 4 and 6) were chosen to be representative of the range of issues evident within the study section (Figure 4), with these then flown at a lower altitude during the second field campaign ( $40\pm 2$

m). This lower elevation resulted in higher density of points within the three reaches. DEMs and hydraulic models were produced for these reaches (see 2.3.2).

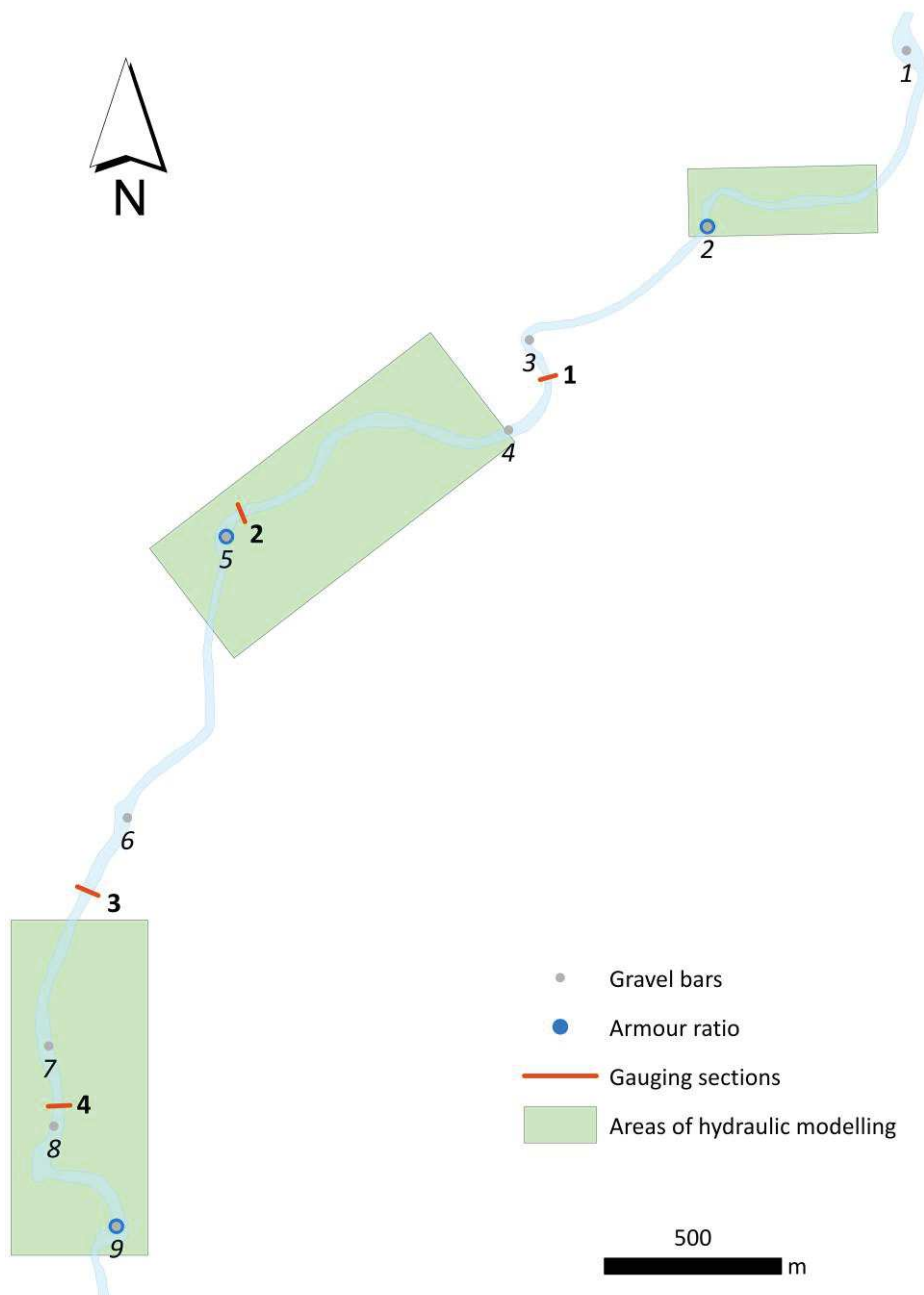


Figure 3. Locations of the detailed study reaches and discharge gauging cross-sections.

Point clouds were produced from overlapping the UAV-derived images using *Structure-from-Motion (SfM)* photogrammetry. Detailed description of the workflow for this can be found in Westoby *et al.* (2012) and Marteau *et al.* (2016). The software AgiSoft® PhotoScan allowed the production of orthophotos and high-density point-clouds, as well as the assessment of errors in the 3D models. In order to determine the quality of the outputs, 3D errors were computed from ground control points that were georeferenced using a d-GPS.

Precision and accuracy of the SfM point-cloud were very good for the model created at reaches 1 and 6 (<4 cm, Table 3) because the GPS was used in 'rtk' mode. The model created

for reach 4 was of lower quality because of technical issues related to the GPS (GPS had to be used in static mode, and hence precision was approx. 35 cm, Table 3).

Table 3. Registration, precision and accuracy of the SfM photogrammetry workflow outputs.

	registration (m)		precision (m)		accuracy (m)	
Reach 1	X	0.0059	X	0.0094	X	0.0081
	Y	0.0102	Y	0.0158	Y	0.0131
	Z	0.0030	Z	0.0077	Z	0.0062
	3D	0.0122	3D	0.0200	3D	0.0185
Reach 4	X	0.3234	X	0.3651	X	0.2700
	Y	0.1718	Y	0.1969	Y	0.1607
	Z	0.0920	Z	0.1155	Z	0.0908
	3D	0.3776	3D	0.4307	3D	0.3503
Reach 6	X	0.0117	X	0.0177	X	0.0144
	Y	0.0209	Y	0.0321	Y	0.0252
	Z	0.0129	Z	0.0239	Z	0.0204
	3D	0.0272	3D	0.0438	3D	0.0377

Point clouds were composed of 456 points/m<sup>2</sup> on average, providing potential information as detailed as the grain scale. The main drawback of the *SfM* photogrammetry technique when surveying rivers is the difficulties in acquiring data for submerged areas. Indeed, the technique is based on optical images for which water is an issue (high reflectance of sunlight, turbidity, surface roughness, etc.). Nevertheless, it is possible to extract, within a given range of accuracy, some information from the *SfM*-derived point cloud with the help of field-based calibration of water depth. To do so, a total of 160 locations within the wetted channel were surveyed using d-GPS to (i) estimate the quality of underwater topography from the aerial survey, and (ii) provide some calibration to improve the results if needed. All GPS measurements were made in rtk mode and had an average 3D error of 0.05 m.

Results (Figure 4) show that underwater estimates from *SfM* photogrammetry are rather robust ( $r^2 = 0.90$ ) and do not require calibration ( $y = 0.99x$ ). Average error (i.e. root mean square error, RMSE) is less than 8 cm and in the same order of magnitude than errors inherent to the model (Figure 4). Thus, the DEMs constructed from the aerial images can be used as the topographic 'layer' for hydraulic modelling with confidence.

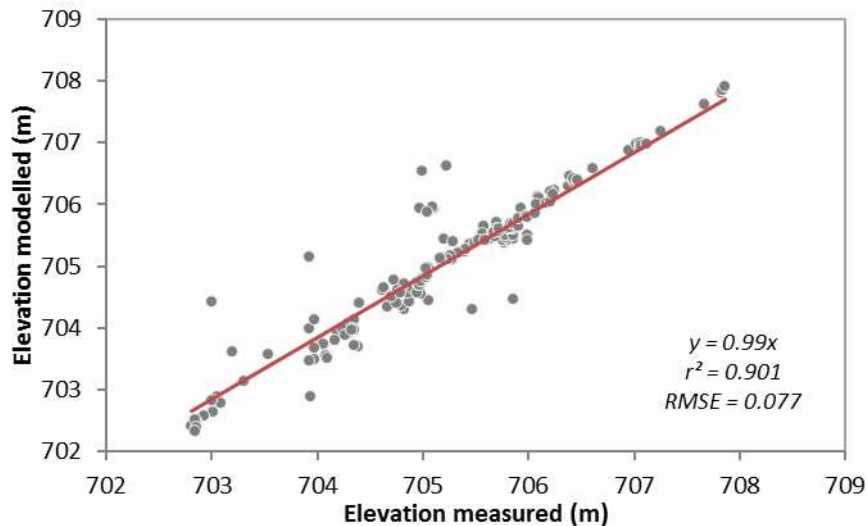


Figure 4. Relationship between measured and modelled elevations in submerged areas.

### 2.3.2 Hydraulic cross-sections and models

Hydraulic survey cross-sections were established in four locations (Figure 3). These were chosen to extend across most of the study section, and be wadable at moderate flows. Discharge was gauged across each of these using the velocity-area method, with velocity measured at  $0.4 \times$  depth (from the bed) at points 1-2 m apart (depending on channel width). All gaugings were made on 8 February 2018.

Average discharge across the four sections on the survey day was  $5.97 \text{ m}^3 \text{ s}^{-1}$ . Maximum velocity at this discharge was approx.  $1.4 \text{ m s}^{-1}$  while maximum depth was approx. 1 m (Figure 5). Despite tributaries entering within the study section, there was no marked increase in discharge in the downstream direction between sections. Thus, tributaries contributed relatively little and flow accretion over the 5.2 km river length was minimal. These flow gaugings provide hydraulic data for calibration of the hydraulic models.

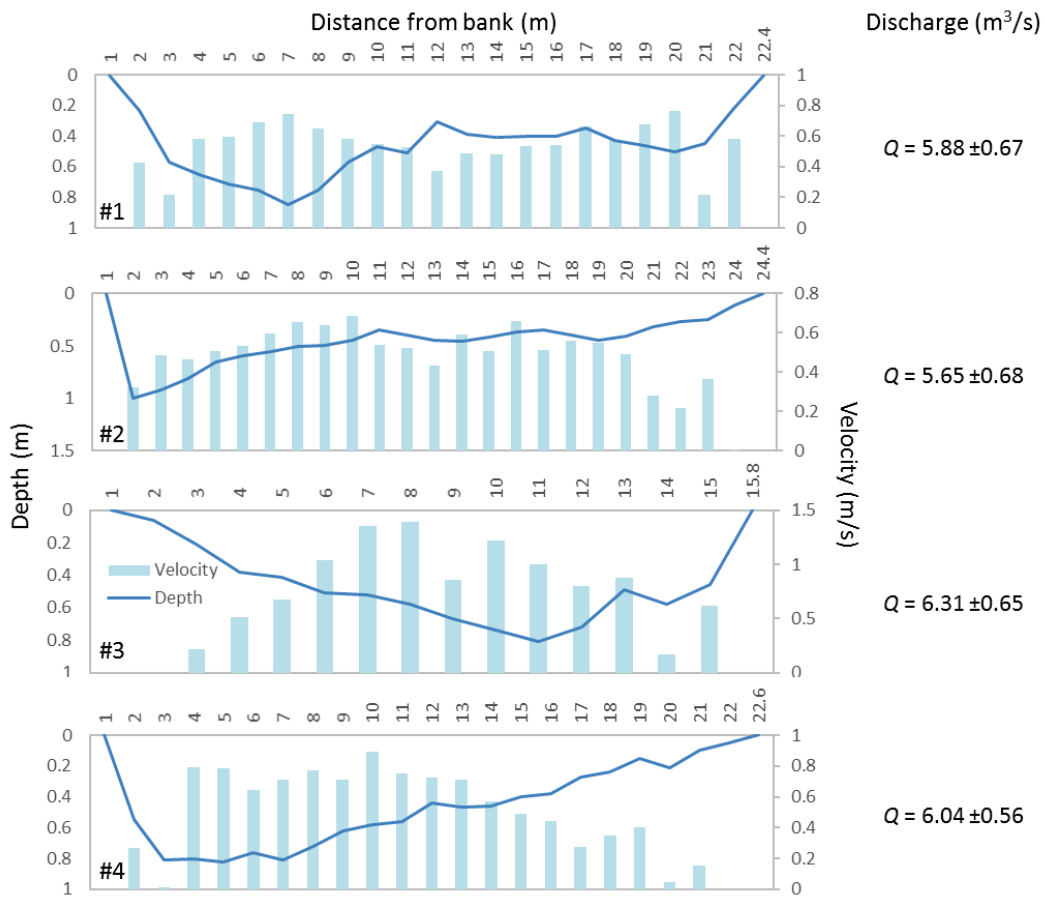


Figure 5. Depth and velocity recorded during flow gauging, and estimated discharge ( $\pm$  uncertainties).

There is a wide variety of models available for the hydraulic modelling of rivers, from simple 1D to very complex 3D models, either commercial or open-source and freely available. The choice was made to use HEC-RAS® 2D, a free software developed by the U.S. Army Corps Engineers (US Army Corps of Engineers, 2018) and which is increasingly being used in the literature.

Hydraulic modelling was undertaken based on the bankfull concept. Bankfull discharge is important as it is the water stage for which energy generated by water is maximised over the wetted perimeter. Above bankfull, flow is spread over the riverbanks and energy is partly dissipated beyond the active channel. Given the purpose of the study, the bankfull concept offers an appropriate approach to investigate the interaction between flow hydraulics and bank erosion. HEC-RAS® 2D was used to simulate flow hydraulics (velocity, shear stress etc) at bankfull flow.

### 2.3.3 Grain-size of bed surface sediments

Sizes were assessed in two complementary ways: information at the morphological unit scale was collected using the Wolman pebble count method, while patch scale (approx. 1 m<sup>2</sup>) data were collected using photographs. Wolman pebble counts were undertaken on nine exposed bars (Figure 7), as close as possible to the hydraulic survey cross-sections. The *b*-axis of a

minimum of 200 clasts was measured at each bar (counts ranged from 202 to 240), with sizes then classified according to the Wentworth Scale. The size of the largest single clast ( $D_{max}$ ) was also recorded for each bar. Grain-size distributions (GSDs) were produced from the pebble counts both to provide a general characterization of surface sediment sizes at the scale of gravel bars and to use to help construct the hydraulic models (for which roughness values are needed) as well as select representative grain-sizes to focus on in assessment of bed stability (i.e. estimating entrainment thresholds of representative size classes).

To complement pebble counts, GSDs were determined for selected patches using photographs processed using Digital Grain Size Project Software® (DGS; Buscombe, 2013). Illustrations in Figure 6 show the resolution and the type of outputs resulting from the use of DGS. Other software is available for 'digital photosieving', but DGS presents the advantage of coping well with the presence of sand and fine sediment (e.g. Figure 6b) and is able to capture bimodal distributions (e.g. Figure 6d).

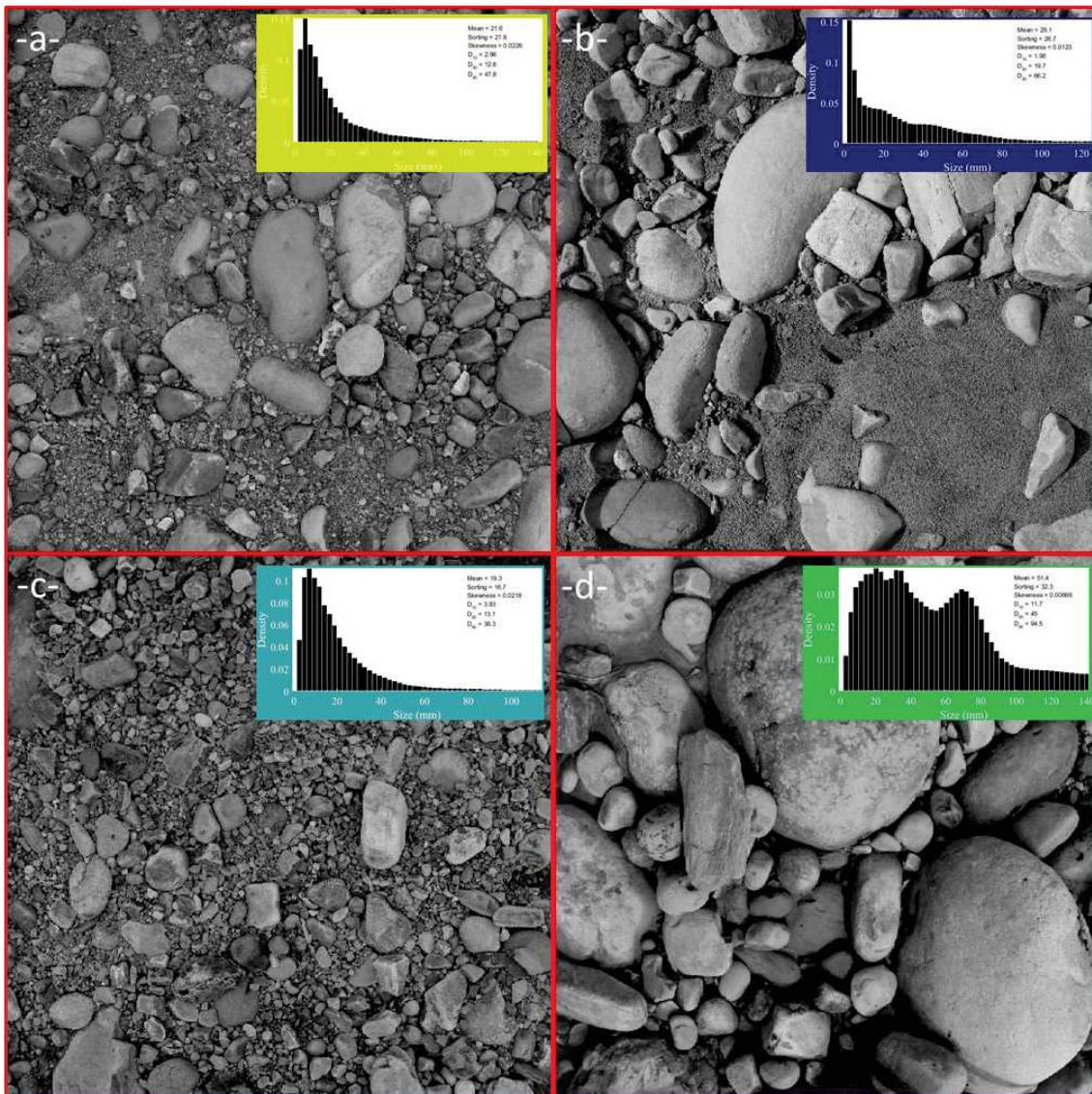


Figure 6. Illustration of different types of sediment patches used for analysis with the DGS software.

	upstream				roadbridge				downstream
Photosieving	P	P	P	P	P	P		P	P
Wolman pebble count	W	W	W	W	W		W	W	W
Painted patch	PP		PP		PP		PP		PP
Gravel bar	1	2	3	4	5	6	7	8	9

Figure 7. Schematic to show the spatial distribution of gravel bars (numbered 1 to 9) and data collected at each one to help characterise riverbed conditions.

### 2.3.4 Bed mobility - painted patches

Additional patches on the bars were delineated using the quadrat and painted, and used to help estimate bed mobility, thus stability. These were painted (i.e. traced) and photographed on the first field campaign and then re-photographed during the second campaign (see example in Plate 1). Grain-sizes were computed using DGS software and compared between dates to determine the sizes of material lost from or accumulated on the patches and assess changes in the GSDs of each patch. When it was evident that scour had occurred, the area around each patch was searched and the maximum displacement distance of clasts was recorded, along with the size of the clast that was displaced furthest.



Plate 1. Photograph of the surface sediments on an exposed bar, River Trusan, 4 February 2018. For scale, all pictures were taken with a ruler visible within the frame.

### 2.3.5 Armouring: vertical variability of bed sediments

The armour ratio (AR) for sediments on each of the bars was estimated. AR is the ratio of the  $D_{50}$  of surface material to the  $D_{50}$  of that for the subsurface layer. As it was impractical to take bulk samples away from the site for sieving and weighing (the standard approach for calculating AR), the median size of material in the surface and subsurface zones was

calculated from digital photographs. For this, a patch on an exposed bar was delineated using a quadrat (1.3 m x 1.3 m) and a photograph taken (Plate 1). Patches free of vegetation were used, to improve the digital size characterization of grain-sizes. All clasts containing paint (by definition, surface material) were then removed, exposing the shallow subsurface (paint-free) layer. A photograph was then taken of this subsurface material. The  $D_{50}$  of material in each layer was calculated using the DGS software (Buscombe, 2013). AR is given here for general contextualisation of the results; care should be taken when interpreting these values, given that they were computed from photographs rather than empirically and so may be subjected to certain bias.

### 2.3.6 Field-based observations and assessment of bank erosion

Ground photographs were taken during the walk-over survey in addition to field notes and personal observations. These were used for the visual assessment of bank erosion, which was grouped into 4 categories – ‘severe’, ‘high’, ‘mild’ and ‘no’ erosion. The orthomosaic generated from aerial images (average resolution of 1.5 cm) was used to map the distribution of erosion along the 5.2 km, coded according to the same categories. Ground photographs were also used to determine riparian vegetation density.

## 3 Findings

### 3.1 Rainfall trends

The Long Semadoh weather station data supplied by DID (which consisted of monthly values) contained missing values. Sometimes whole years were missing from the series (e.g. 1954, and the period 1956-62 inclusive were missing) while for other years some monthly values were missing. These missing data prevented a full time-series analysis of the complete range of rainfall statistics. Nevertheless, it is possible to assess patterns in some potentially insightful rainfall statistics over a 67-year period, namely the mean maximum daily rainfall (i.e. the average of the maximum daily values recorded in each month of each year) and the total annual rainfall (Figure 8 and Figure 9).

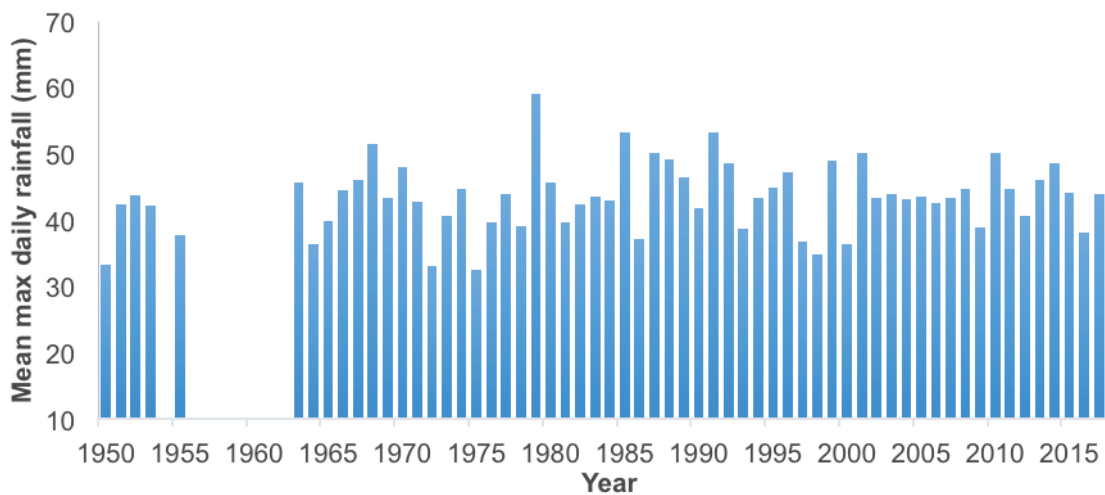


Figure 8. Mean maximum daily rainfall at Long Semadoh for the 1950-2017 period.

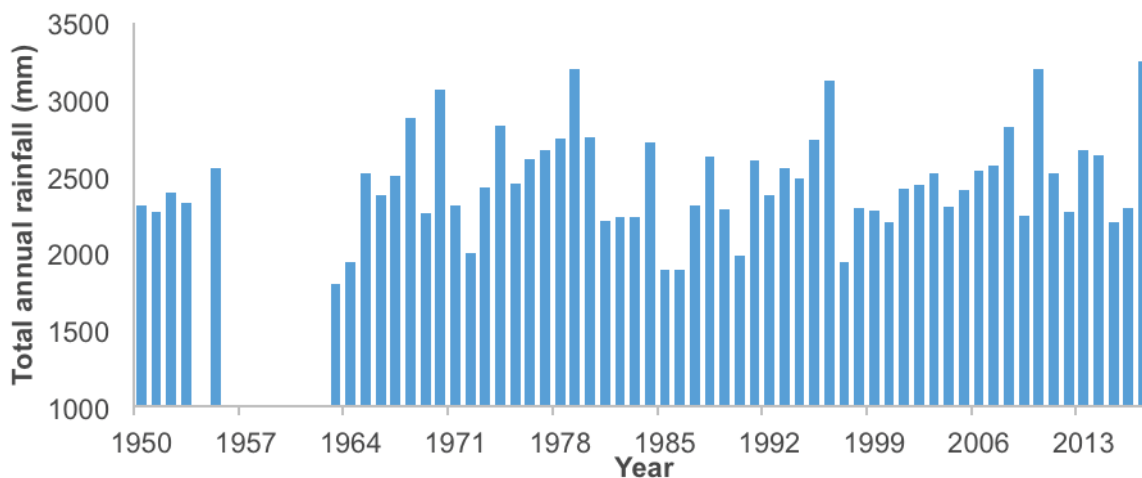


Figure 9. Total annual rainfall at Long Semadoh for the 1950-2017 period.

Statistical analysis of the trends in maximum daily and total annual rainfall was undertaken using a Mann-Kendall test. The tests revealed no autocorrelation within each dataset (i.e. no

cyclic patterns) and no increasing nor decreasing trend between 1963 and 2017 (total annual precipitation:  $\tau = 0.0667$ ,  $p$ -value = 0.477; mean maximum daily rainfall:  $\tau = 0.0264$ ,  $p$ -value = 0.783). As such, any change in hydrology that may have been observed in the Upper Trusan cannot be related to a change in rainfall; it is likely to be caused by other factors such as activities within the catchment (changes in land use, deforestation, flow regulation, alteration of the floodplain retention properties, etc.).

As outlined in Section 2.2.1, discharge is not gauged at Long Semadoh and the data series for the next downstream station (Long Tengoa) is poor. Given the scarcity and dubious quality of the data, it would be unwise to apply any formal statistical tests (these would imply confidence in the data beyond that which we have) so we have simply converted the water level values to discharge and plotted these, to allow a visual inspection of patterns. The most complete record is for the period 2005-2010.

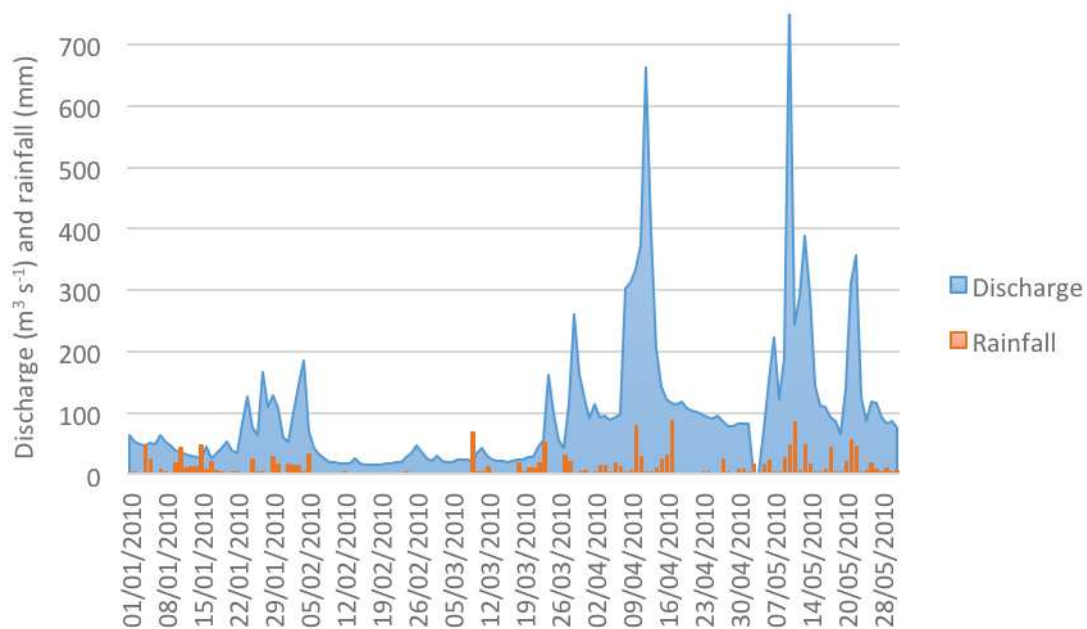


Figure 10. Example of channel discharge response to rainfall at Long Tengoa for the first five months of 2010. All values are daily.

The mean discharge at Long Tengoa for the period of record is  $108.7 \text{ m}^3 \text{ s}^{-1}$ . In general, the river here (a location approximately two thirds of the way down the basin) responds quickly to precipitation (Figure 10), with sharp rising and recession limbs of event hydrographs. In turn this might suggest abrupt changes in hydrology could be expected if landcover changes occur in the catchment. It can be expected that in the headwater areas around Long Semadoh, the river responds even more rapidly to rainfall. While discharge data are not available to support this statement, rapid changes were evident during the fieldwork periods (with stage rising by approximately 1 m within an hour or two).

Looking at the discharge time-series overall (Figure 11), it is very hard to suggest that any major change in the hydrology of the river has occurred. There appears to be a weak trend of

reducing discharge of the first two years, but the subsequent data gap means that it is unclear whether this continued/was sustained, or whether it was simply part of cyclical behaviour. The last two years of the record (2009 and 2010) show some suggestion of a trend of increasing baseflows; this is less evident in the discharge data than the stage values, and may reflect issue with the transformation of stage to discharge (i.e. rating curve). To help assess any changes in hydrological behaviour, the number of days that discharge exceeded 1.5 times the long term mean discharge (flood events) was assessed for different periods, with this then expressed as % of time. The cumulative percentage of time during the first continuous period of record (1999-2001) that the river was experiencing flood events was 17.2%, while the value for the most recent period of record was 20.1%. These values suggest that the recurrence of flood events has not changed substantially. Unfortunately, data for the period within which increased flooding and erosion have been reported by local communities (the last 5 years or so) are not available, so it is not possible to assess whether any changes in flood frequency have occurred. The fact that we can say little with any great confidence helps stress the importance of good quality long term data. In particular, having information on discharge at Long Semadoh would be extremely useful in the future (for which see Recommendations section).

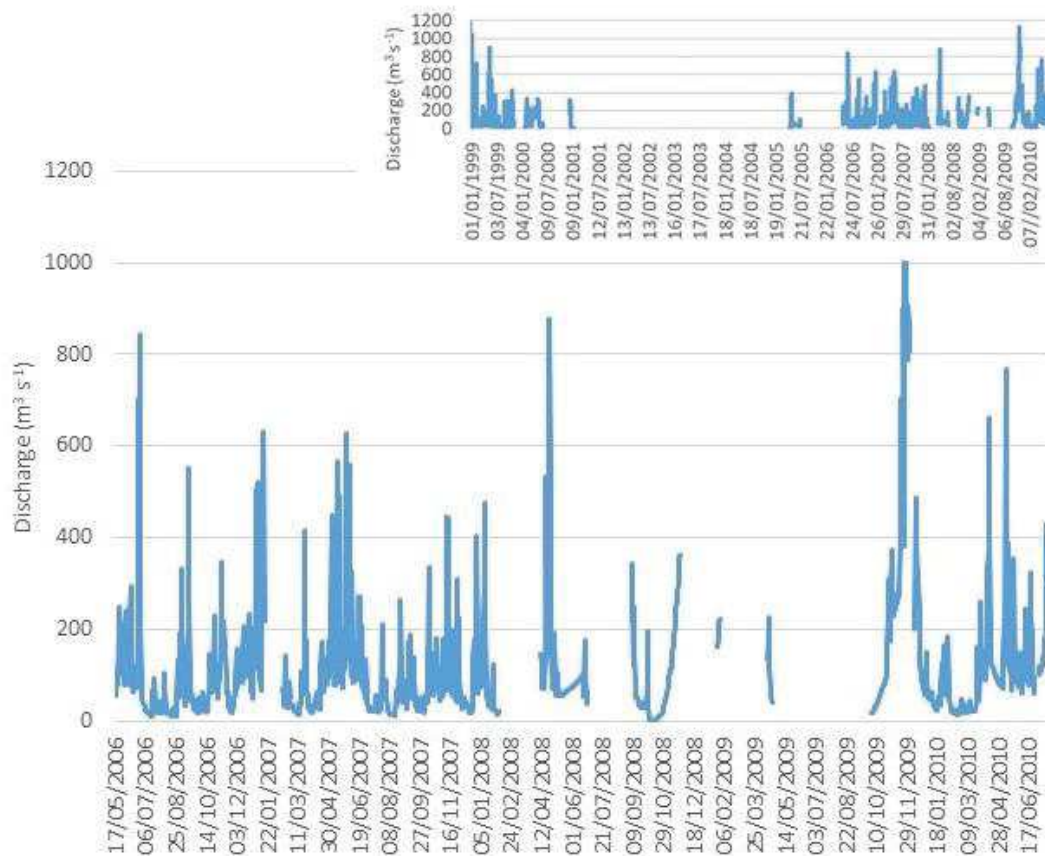


Figure 11. Available discharge data for Long Tengoa. Inset shows the whole period of record (1999-2010) while the main part of the figure shows the relatively complete recent four years of record in more detail.

## 3.2 Land cover and land use changes

### 3.2.1 Tracks and roads

Initial observations of the satellite images for the Trusan suggest that parts of the catchment are crossed by a rather high density of tracks, although less than seen in some neighbouring catchments. It was thus hypothesised that the construction of some of these tracks may be in part responsible for the production of fine sediment and the increased turbidity seen in the Trusan - tracks and roads are well known not just to contribute to the high fine sediment loads seen in many tropical rivers but also to modify connectivity (i.e. the transfer of water and sediments through the different compartments of a system). Overall track length is used here as a metric to represent the potential contribution of access tracks to fine sediment loads.

Analysis of data from 1985 onwards reveals that little has happened since 2005 (Figure 12). Most of the tracks (70%) seen today were built between 1988 and 2001, with these primarily being access routes linking the villages. There was an increase in total track length from 39 to around 54 km between 2001 and 2004, with these new routes cut through forest. No major track construction within the last decade or so is evident from the satellite images (<1 km of new tracks added). Tracks are concentrated along (1) a primary axis of traffic to and from Long Semadoh village, and (2) in the northern part of the catchment. Neither of these seem to be associated with deforestation or land clearance as might have been expected. The eastern side of the catchment remains largely devoid of access tracks and roads.

Overall, tracks have increased markedly in the last 30 years, though with slower rates of increase in the last decade. Even so, special attention needs to be paid since the response of a system to a disturbance may not be immediate (what is called "the reaction period" as per Petts and Gurnell, 2005).

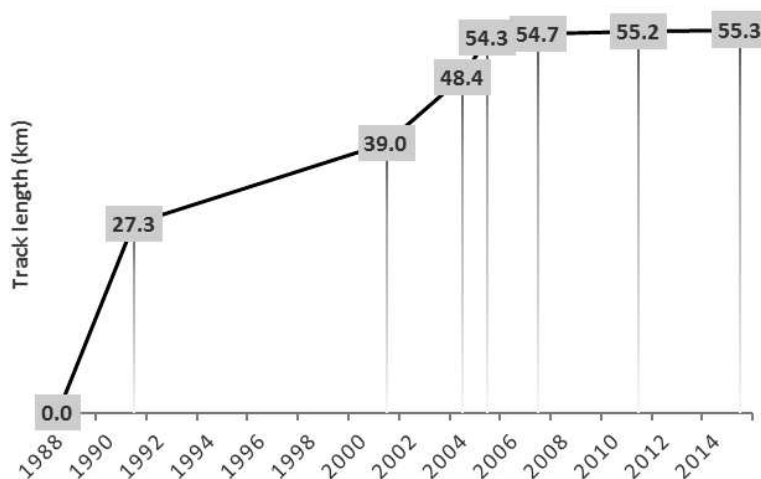


Figure 12. Changes in the total length of tracks and roads in the upper Trusan catchment. Data derived from Landsat satellite images and Earth Engine.

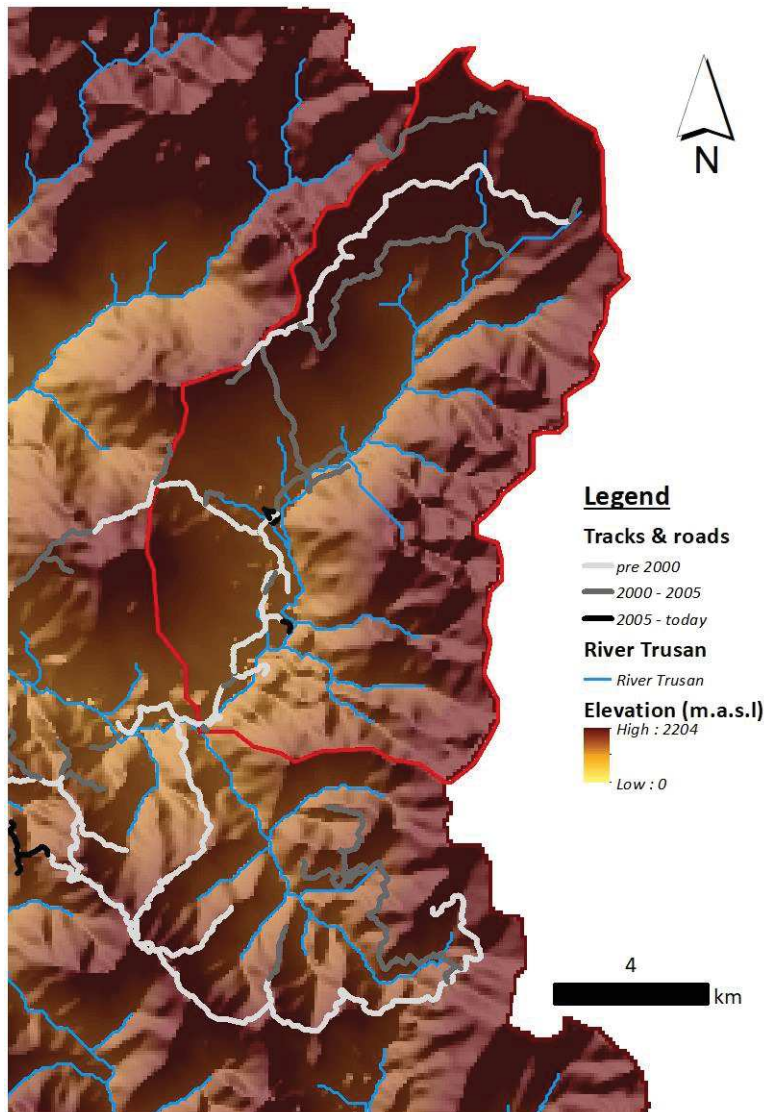


Figure 13. Tracks and roads built within the Upper Trusan catchment. Note that most tracks follow either (i) the stream network or (ii) topography.

### 3.2.2 Forest clearance and disturbance

Land cover change was assessed for the period 2007 to 2017 (Figure 14). Forest still covers approximately 95% of the area of Upper Trusan catchment, with overall rates of deforestation and disturbance (e.g. selective logging, partial cutting) lower than observed in other sub-catchments within the broader Trusan basin (pers. obs.) and across Malaysian Borneo in general (Bryan *et al.*, 2013). In fact, there are places within the upper Trusan sub-catchment where no disturbance was observed (white areas, Figure 14).

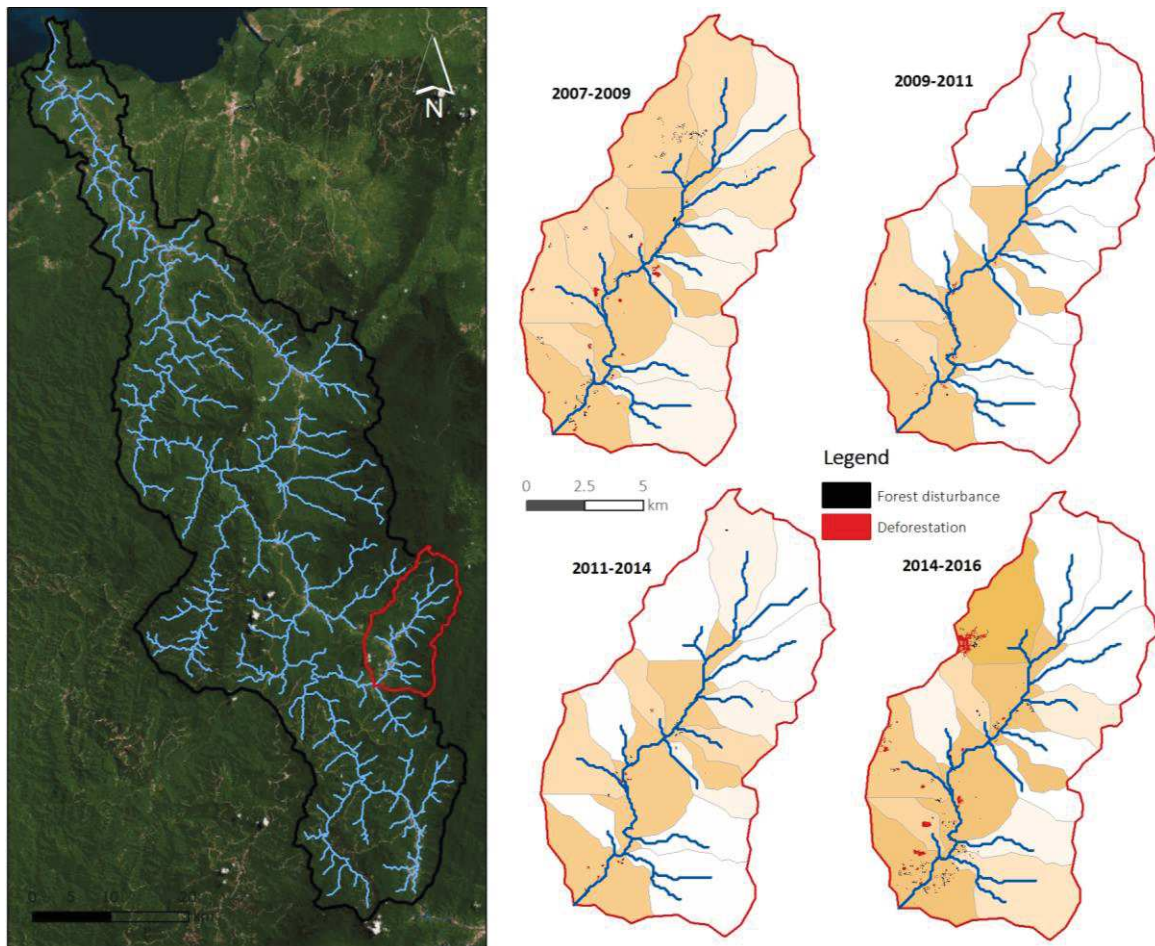


Figure 14. Forest clearance and disturbance within the upper Trusan catchment, determined using CLASlite. Data are shown by sub-catchment, with disturbance coloured according to the percentage of land that suffered from alteration (disturbance and deforestation together). Satellite image on left from ESRI Database. Satellite images used for analysis from Landsat imagery.

Deforestation was evident between 2007 and 2009 in the vicinity of the river, while numerous localised isolated cases of forest disturbance were apparent on the western side of the catchment. These disturbances were close to tracks and may have been associated with track maintenance or local logging. No major deforestation was evident between 2009 and 2014, although some logging activity can be identified locally around the river (i.e. within the floodplain). The heaviest logging activity, despite very localised, was observed between 2014 and 2017, with this also concentrated on the western side of the catchment as well as within the river floodplain. Important deforestation occurred in the north-west of the catchment within the Sungai Rengir sub-catchment. This is notable as being where villagers from Punan Trusan reported increased deposition of sand and fines in their rice paddies.

The NDWI index extracted from Landsat images shows a slight increase in wetland surface over the 10-year period between 2000 and 2010, which can be estimated as being rice paddies. The apparent increase in 2016 (Figure 15; around 0.5 km<sup>2</sup>) is not significant, and may be caused by either artefact (e.g. wetter weather conditions) or linked to the higher exposure

of wetlands/paddies. However, the coarse resolution of the images (i.e. 30 m) does not allow the resolution of such small changes.

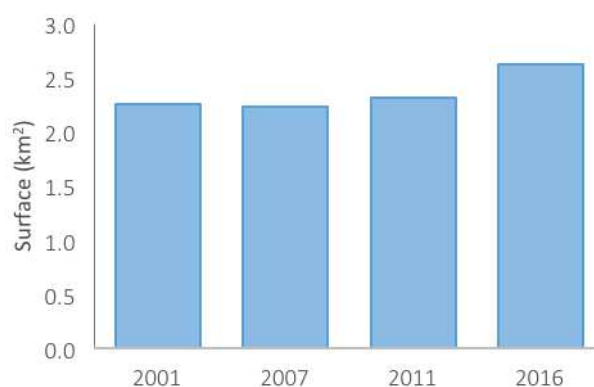


Figure 15. Estimated surface of rice paddies (may also include wetlands) within the corridor of the Upper Trusan River.

#### Key points

1. The absence of good quality data makes it hard to assess whether any long-term changes in river discharge have occurred, but rainfall data indicate that there has been no marked change in precipitation since 1963 at the Long Semadoh weather station.
2. Though many new tracks have been built within the last 30 years, there has been no marked increase within the last decade.
3. While not as marked as in other parts of Malaysian Borneo, there has been localised forest clearance and disturbance in the Upper Trusan. This is particularly visible in the last 3-4 years and mainly concentrated within the Sungai Rengir sub-catchment.
4. Analysis of Landsat images indicates that the extent of rice paddies has remained stable over the last few decades.

### 3.3 Inventory of riverbank erosion within the Upper Trusan catchment

Using a combination aerial and ground photographs, as well as notes from the walk-over survey, a map of erosion was produced (Figure 17). This used a simple classification and basic colour-coding, running from no erosion (0, blue) to severe erosion (3, red), and based on visual assessment of bank stability, height and extent of bank failure and estimated risks of further increase in erosion (considering channel geometry and position of the bank relative to main flow veins). This task was undertaken to provide a primary understanding of erosional issues observed in the field, in order to prioritise the subsequent surveys and modelling exercises. Figure 18 illustrates some of the types and magnitude of erosional issues observed during the survey.

### 3.3.1 Severity of bank erosion

Most of the more extensive problematic areas (red and orange) are located in three main areas: the uppermost 1 km, the lowermost 0.5 km of the study section, and approximately 0.5 km on each side of the road bridge location about half-way through the study section (Figure 17). Between here there are some isolated pressure points, but much of channel has little or no erosion (green and blue). When looking at the total length of banks (i.e. both left and right banks of the study section), the majority (70%, 7.8 km) suffer no or only mild erosion (Figure 16); these could be considered as non-problematic under natural conditions. A remaining 3.3 km of bank was classified as either suffering high or severe erosion. These primarily concern areas with no riparian vegetation, although 2 different conditions were identified; cases where the absence of trees renders riverbanks highly erodible and exposed, and cases where land clearance (usually on slightly higher ground) has caused landslides which are now being eroded by the river, causing important deposition of fine sediments further downstream. These different scenarios are further detailed in the sections below.

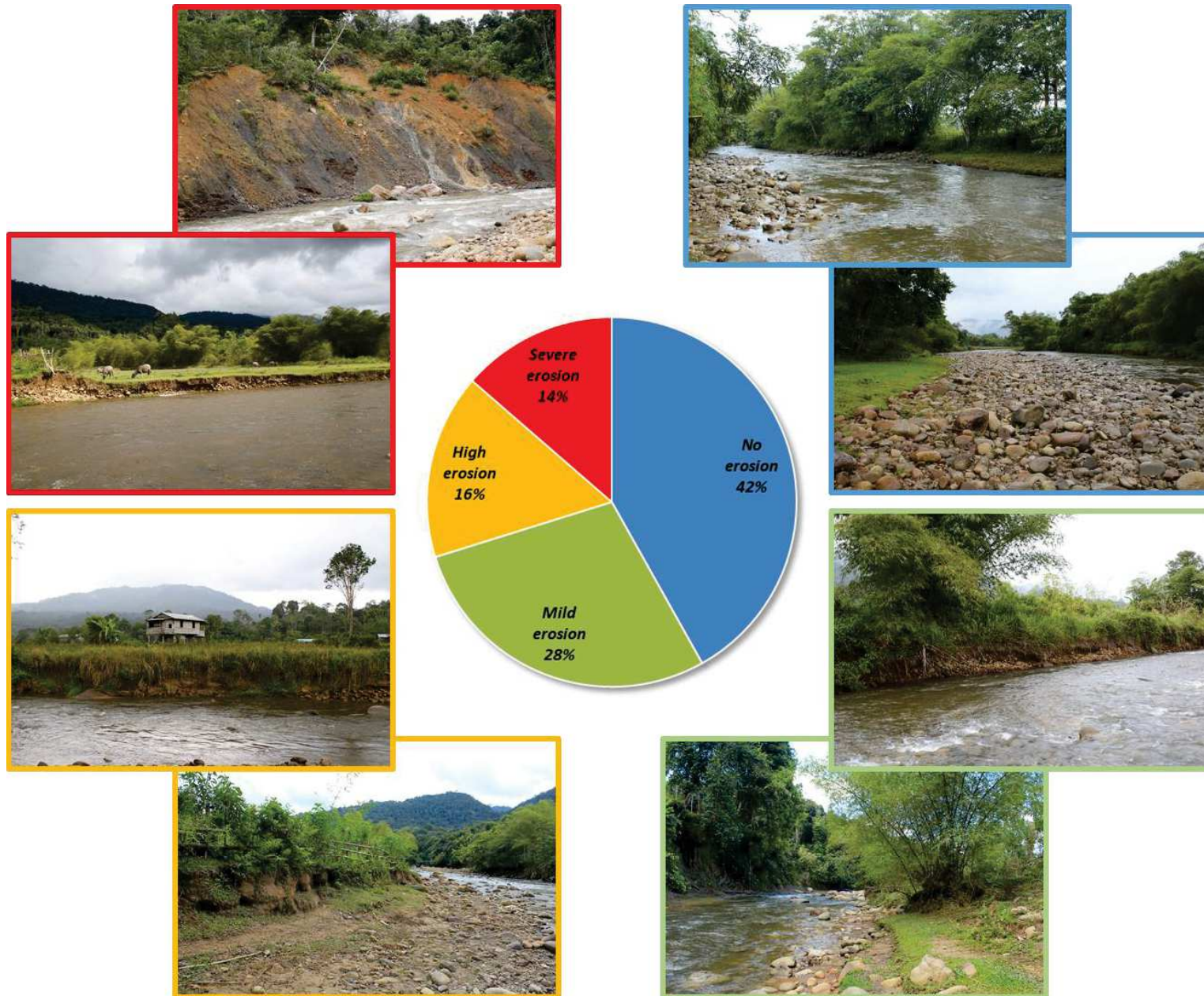


Figure 16. Proportion of the different categories of bank erosion observed in the upper Trusan (see also Figure 17).

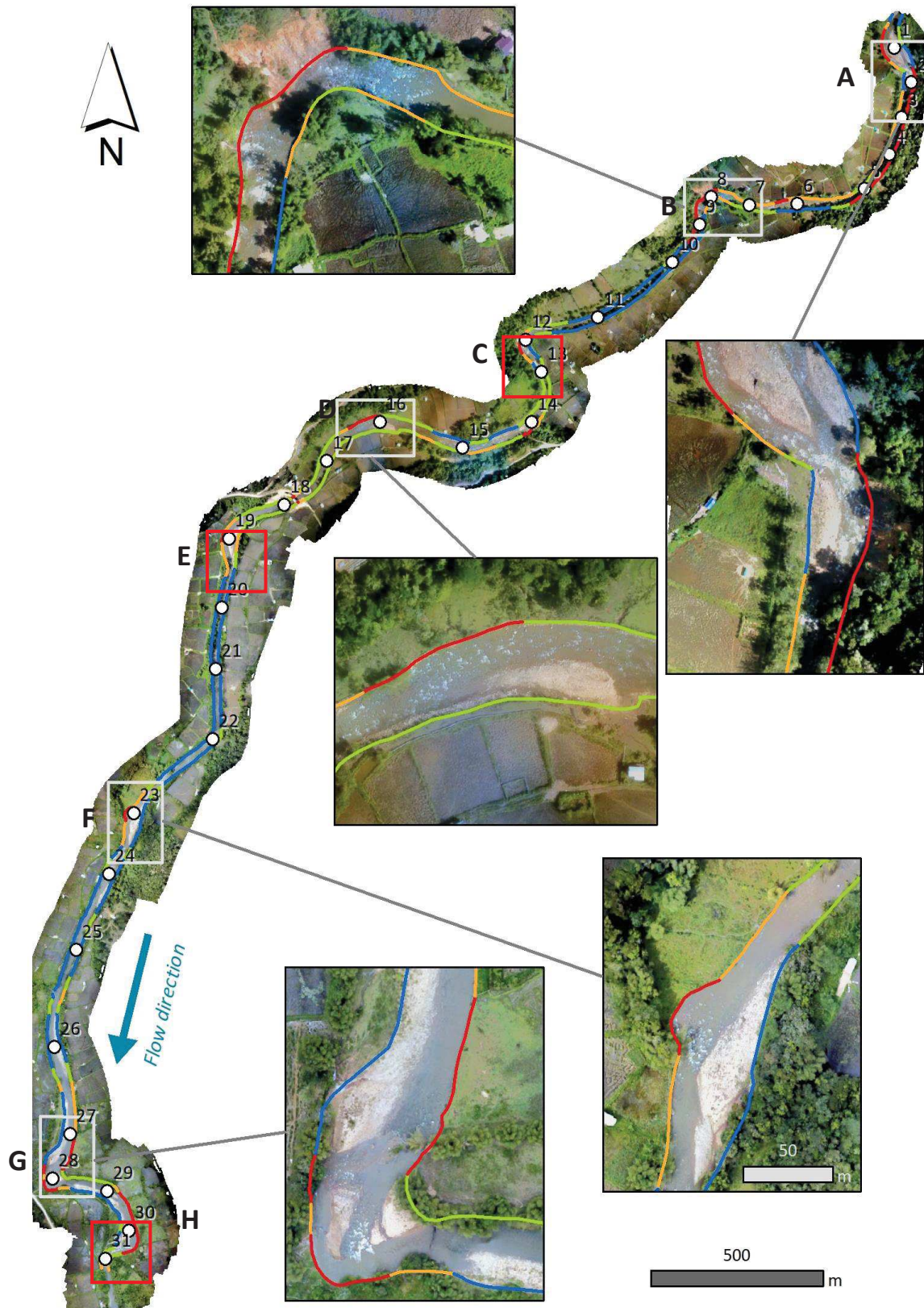


Figure 17. Map of erosion in the study section of the Upper Trusan. Red and white boxes show areas of particular concern. Red = severe erosion, orange = high erosion, green = mild erosion, blue = no erosion. Examples of areas of concern (the white boxes) are shown in the zoom-ins; areas in red are not shown as zoom-ins simply due to space, but are discussed the main text.

Several areas were identified as being problematic. These are detailed below and illustrated in Figure 17 and Figure 18.

1. The uppermost section (A) shows some erosion on the right bank adjacent to the gravel bar, with bank retreat of 3 to 7 m estimated for the period 2015-18 (Figure 18e; based on Landsat images for the two years). Also, the river here is slowly eroding the forested left bank, with an estimated 10 m bank retreat; appendix Km0.1 and Figure 18e). There is also a major landslide on the left bank, caused by forest clearance on the valley side. Due to the location of this section, there is no direct impact on human settlement. Downstream, between sections A and B, the entire left bank is subject to severe erosion. This is due to intervention in the channel - large boulders have been moved from the right bank towards the centre of the channel in order to prevent erosion of rice paddies, influencing flow hydraulics and conveyance. The consequences are limited by the high resistance of the left bank, although these are likely to remain for a long period (appendices Km0.2 & Km0.4). This area is also subject to trampling by buffalos (appendices 6 & 8) which compact and facilitate erosion of already exposed banks.

2. Section B shows a large landslide on the right bank due to land clearance (appendix Km0.9). The area subject to slope degradation increased by 50% (from 1000 m<sup>2</sup> to 1500 m<sup>2</sup>) between 2015 and 2018 (based on analysis of aerial images). The consequences of this landslide are directly visible on the gravel bars immediately downstream, with large lenses of sand and fine deposits observed on top of coarser material.

Between sections B and C there is more or less continuous tree cover along the riparian zone. This provides bank stability, with erosion more or less absent (classified as blue; see also appendices Km1.1 & Km1.4).

3. Section C has similar issues, with a landslide on the right bank and visible and extensive depositions of fine sediment directly downstream.

Downstream from the landslide in section C, alternate gravel bars provide interesting and ecologically important habitats (i.e. riffle-pool sequences). When reaching the next bend, erosion is visible on the left bank opposite a large gravel bar, although this does not threaten valuable land (appendix Km1.8). Modification of the channel is visible on the right bank after this erosion, where locals have moved large boulders towards the centre of the channel in order to create an intake of water to irrigate rice paddies (appendix Km2.0). The main geomorphic consequence of these alterations is the removal of a gravel bar, observable from the comparison between aerial images from 2015 and 2018.

4. Section D illustrates one of the major issues evident from the field surveys. With the objective of protecting a road bridge (near point 18 in Figure 17), a 1.5 km section of river has been channelized, with very coarse material pushed up onto each side of the channel to stabilise/protect the banks (appendix Km2.5). To do so, an access routeway was constructed on the left bank across a gravel bar (see appendix Km2.3). This produced a very compact

gravel bar which diverts flows towards the opposite bank. The consequences of channelization and related access works are 'textbook' effects of poor river management: the outside of the first bend downstream from the access route now suffers from severe erosion (typically undermining the bank), with most of the riparian vegetation removed or about to collapse into the river (shaded area in Figure 18d). Based on analysis of time series images up to 12 m of bank retreat is evident in the last 3 years (2015-18), with an estimated 790 m<sup>2</sup> of land eroded and lost over this period.

5. The channelization has created a very uniform channel cross-section (appendix Km2.5). Flows here are very uniform and fast during high discharges (observed once in the field), and so unlikely to provide suitable habitat for fish or invertebrates. Despite the recent channelization, it is already evident that the river is beginning to 'recover' or readjust, with e.g. some natural geomorphic features such as lateral gravel accumulations apparent during the field surveys. This rapid adjustment shows the futility of this type of engineering in a high gradient section of river.

6. Immediately downstream from the road bridge, bank modification and stabilisation continues for approximately 70 m on the right-hand side, where the vegetation has been cleared to store gravel extracted from channelized section; the area is used to park diggers and trucks. In this area, approx. 2.5 to 7.5 m of bank retreat is evident in the aerial images (from 2015-2018; see appendix Km 2.7 and beginning of Km2.8).

7. In Section E, the acceleration of flows caused by the canalised section, together with the presence of a well-developed gravel bar on the left-hand side of the channel, has generated important erosion on the meander (Figure 18e and appendix Km2.8). Although the banks have remained rather stable, much reworking of the previously existing gravel bars has occurred in the last 3 years and may have an impact locally in the future.

The 650 m section of river downstream from here shows low risk of erosion (appendices Km3.0 to Km3.4). The riparian vegetation is well developed and preserved on both sides of the channel, and a few large boulders and various geomorphic features are present to dissipate and disperse water energy.

8. In Section F, the absence of riparian vegetation (Figure 17 inset and appendix Km3.7) is responsible for the erosion observed on the right bank. Up to 18 m of bank (i.e. estimated 980 m<sup>2</sup> of land) has disappeared in this bend since 2015 (Figure 14c). At the moment this does not directly threaten valuable land, but if erosion continues it is likely that some rice paddies on the right side of the channel will be lost to the river.

Downstream from section F, for c. 600 m the river shows only localised signs of erosion (appendices Km3.9 to Km4.4). These are intrinsically linked to a more or less natural behaviour of the river, and a continuous tree cover within the riparian zone allows the banks to resist scour and major erosion.

9. Section G is the next critical point of erosion, where extensive bank undermining is visible on the true left bank (appendix Km4.7 & Km4.8). Up to 18 m of bank retreat has occurred here since 2015, with an estimated 1360 m<sup>2</sup> of land lost (Figure 18b). This land was primarily used as pasture, which is arguably less valuable than rice paddies. Nevertheless, the complete absence of riparian vegetation along section G means that erosion here is likely to continue. In contrast, the gravel bar located on the opposite bank is continuously growing in size and is increasingly being colonized by terrestrial vegetation. Vegetation acts as a binding element and increases the energy necessary for gravel to be entrained, thus decreasing the probability of natural sediment movement. The reshaping of this section has also had consequences for the sharp bend at its downstream limit (erosion on the right bank; Figure 18b and appendix 28) but also further downstream in the most downstream section surveyed (Figure 18a and appendices Km5.0 & Km5.1): here, erosion is evident on the left bank where riparian vegetation is absent and the highly erodible bank material (i.e. old alluvial sediment, deposited by the river in the past) is left exposed.

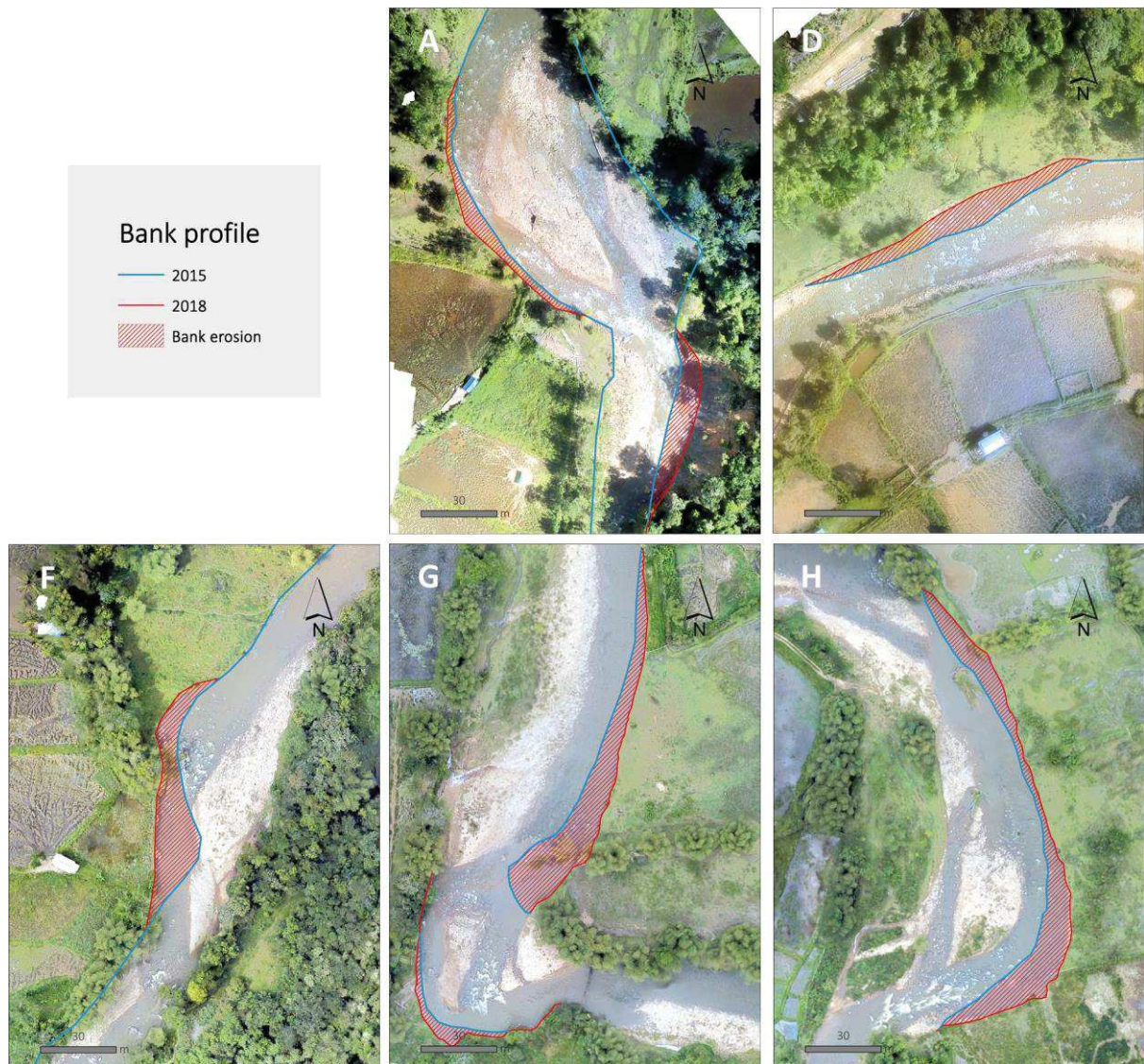


Figure 18. Zoom-ins of the main erosional areas; blue lines represent the position of the bank in 2015, and red lines the position of the banks in 2018.

### Types of bank erosion

The second step in the analysis involved categorising areas of high and severe erosion according to the categories defined by Charlton (2008) (see also the Review document which accompanies this report; Marteau *et al.*, 2018). The purpose of this analysis was to assess the proportion of observed erosion that can be linked to fluvial processes.

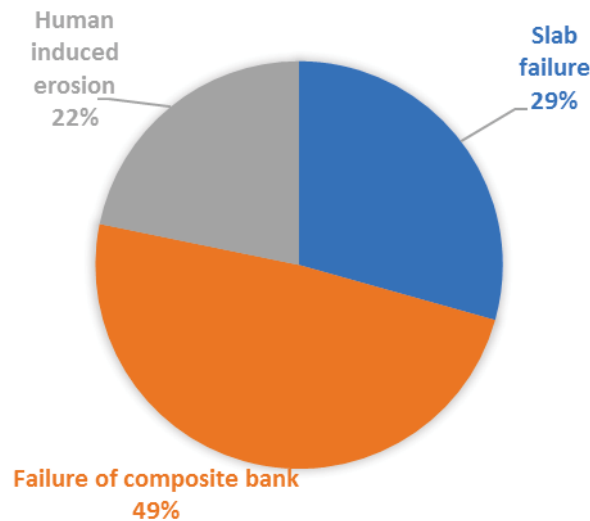


Figure 19. Categories of erosion observed in areas suffering from high or severe erosion. Human induced erosion involves the direct damage caused by diggers or trampling by buffalo. Results indicate that the majority of erosion is caused by the failure of composite banks. This category is often associated with fluvial processes - flow fluctuations, flow competence and bed scouring.

### 3.3.2 Influence of local controls on erosion

Evidence of hydrological change is hard to evaluate because of data paucity and quality. However, assessments of other large (catchment) scale controls (i.e. rainfall, land use, track building, rice paddy extent) presented above suggest that these factors have not changed significantly on recent years. Thus, it is possible that more localised factors may be contributing to the reported increase in erosion.

To assess these local controls, orthophotos and ground-based photographs were used to estimate the density of riparian trees along the study section; density was classified as either (i) no woody vegetation, (ii) sparse vegetation, (iii), dense vegetation (continuous line of trees but narrow width) and (iv) large vegetation (dense and forest-like trees). An additional category was used to identify banks that are protected by large gravel bars for which the importance of vegetation for bank stability is secondary. This assessment of riparian vegetation, together with the classification of erosion (none to severe) was used to study the influence of local controls. A Multiple Component Analysis (MCA) was run on to assess relations between erosion and vegetation. This is similar to the commonly used Principal Component Analysis (PCA), but is suitable for categorical data.

Results from the MCA show that severe erosion is strongly correlated with the absence of vegetation (dots for these two parameters are located close to each other on the graph (Figure 20). Similarly, modification of banks (i.e. alteration by access with diggers or cattle) is statistically associated with high erosion. Conversely, locations with mild and no erosion have their banks protected by gravel bars or dense vegetation. Interestingly, erosion (either its absence or presence) is not strongly correlated with the presence of bands of large trees (i.e. forest-like density); thus, while locations with a high density of vegetation experience limited erosion, having large mature trees does not further prevent bank erosion. To assess whether erosion was generally more prevalent on one bank or the other, 'left' and 'right' were used in the analysis. The fact that dots for these dummy variables plot close to zero-zero (the origin) indicates that when considered along the whole of the 5.2 km section, the degree of erosion is not influenced by which side of the channel a location happens to be on.

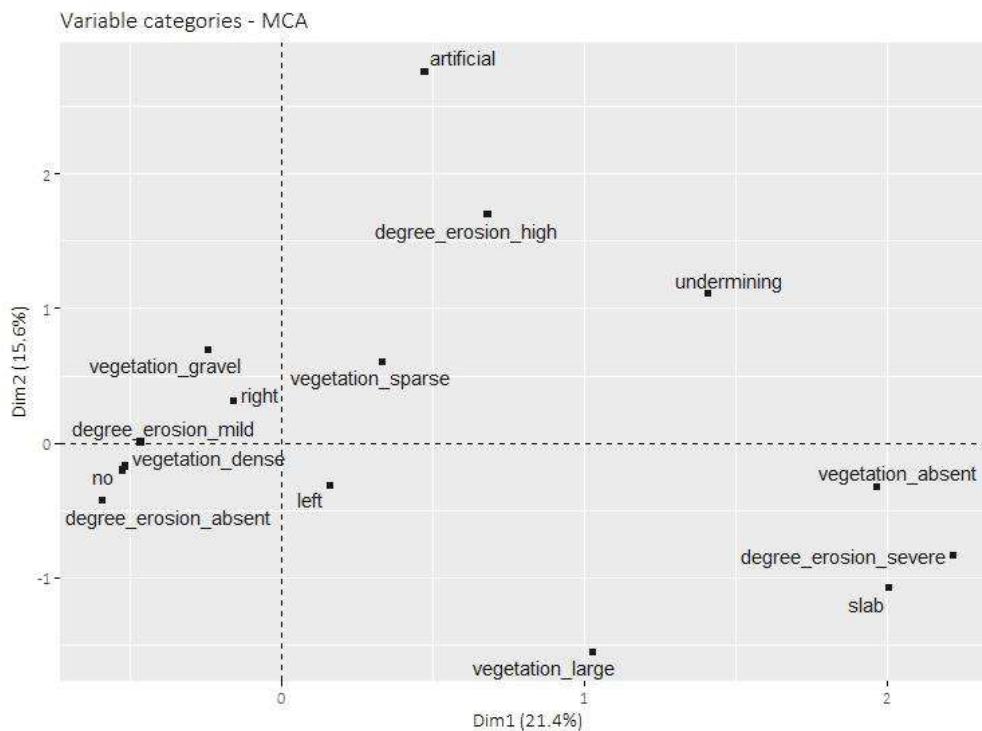


Figure 20. Results of the Multiple Component Analysis of bank erosion data.

#### Key points

1. An estimated 58% of the 5.2 km-long study section shows some form of erosion, with 30% considered as showing high or severe erosion. Erosion is most extensive in the upper and lower parts of the section, but some major isolated areas of erosion occur within the middle section, where two landslides are associated with areas of forest clearance on the steep slopes directly adjacent to the river channel.
2. The spatial sequencing of landcover and channel modification, bank retreat and channel reshaping is evidence of the river constantly responding to pressures: bank stabilisation or channelization in one location leads to increased flow velocity and stream power downstream,

while in other areas reduced stream power has resulted in 'terrestrialisation' of once loose and mobile gravel bars, with associated increased stability of bed material.

3. The multivariate analysis provides overwhelming evidence that clearance of riparian trees is a major factor contributing to observed erosion.

### 3.4 Bed sediment size

This was assessed at different scales; the Wolman pebble count (Wolman, 1954) allows characterisation of particles coarser than 8 mm over an entire gravel bar, while the photosieving method (Buscombe, 2013) provides local but more detailed information and includes the finest range of grain size distribution. The locations of bars where grain size distributions were determined is shown in Figure 7. Based on the pixel size in the images taken the minimum level of detection was between 0.4 and 0.15 mm/pixel.

#### *Wolman pebble count*

Grain Size Distributions (GSDs) measured at the bar scale revealed that the upper half of the study section was dominated by the 32-64 mm size class (large gravels) while the lower part was dominated by the 64-128 mm size class (small cobbles). This difference, however, is not reflected in the size of the large clast found ( $D_{max}$ ), which was smaller in the lower part of the section and larger (880 mm) in the middle (bar 4, Figure 21). The lowest fractions of sediment <8 mm were found where the bars showed few small gravels (class 8-16 mm). Bars 5, 6 and 8 contained large proportions of sediments <8 mm (between 15.5 and 23.7%); these bars are located just downstream from large disturbances, such as landslides (bar 6 and 8) and channel stabilisation, undertaken to protect a road bridge (bar 5). The presence of large volumes of fine sediments on these bars does not seem to influence the grain size distribution of the larger particles; these are thus a direct response to human disturbances.

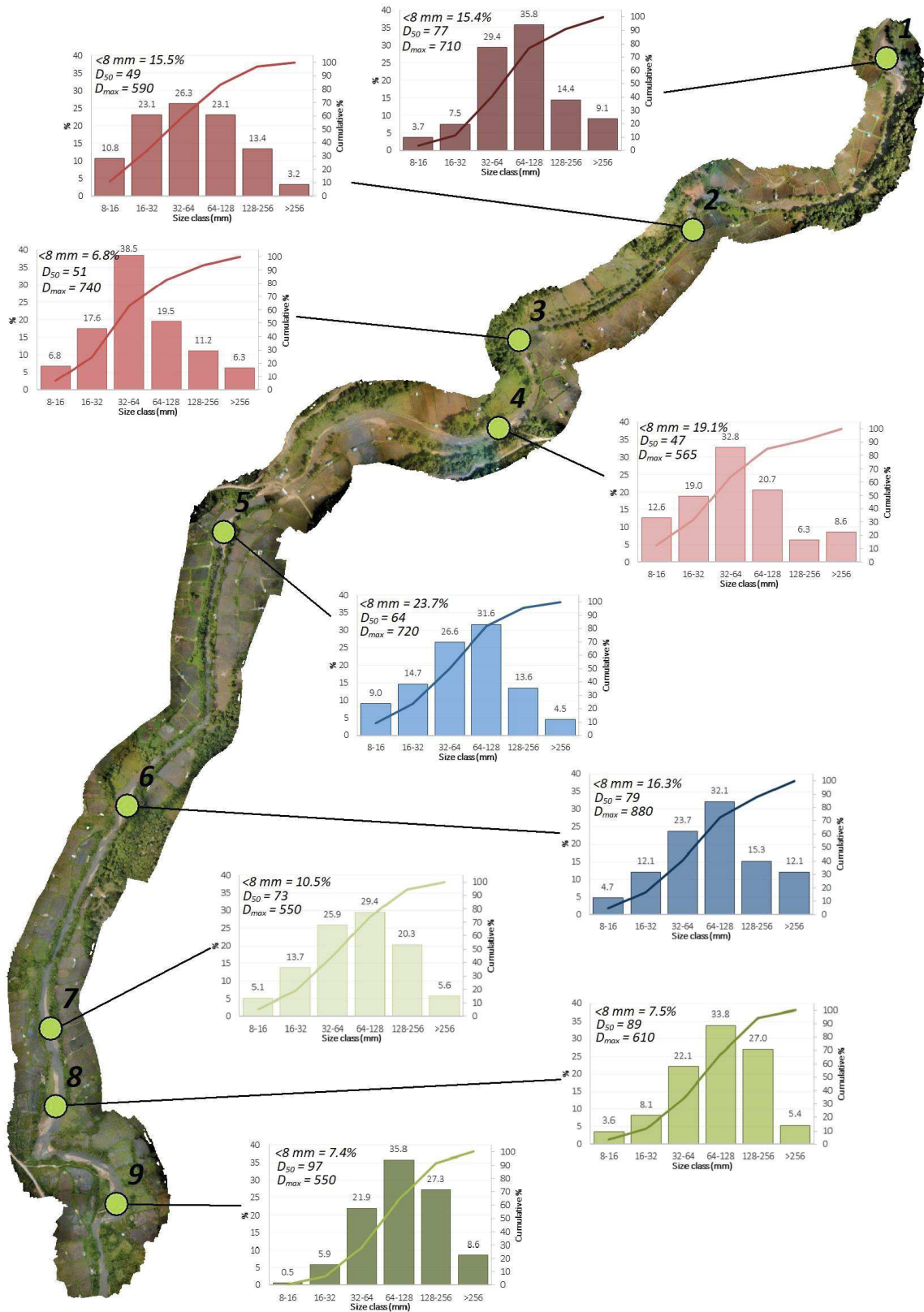


Figure 21. GSDs of the different gravel bars samples along the upper Trusan; with the largest particle measured ( $D_{max}$ ) and percentage of particles smaller than 8 mm.

### Photosieving

Analysis using the digital gravelometric software focussed at the patch scale and incorporated finer sediments in the analysis (i.e. unlike pebble counts, the GSDs produced by the software incorporate material < 8 mm). Results of photosieving (Figure 22) suggest that while the upper and lowermost bars surveyed have different GSDs, there are no clear leaner up to downstream change in sizes; in general there as much variation in GSD across each bar as there is between bars.

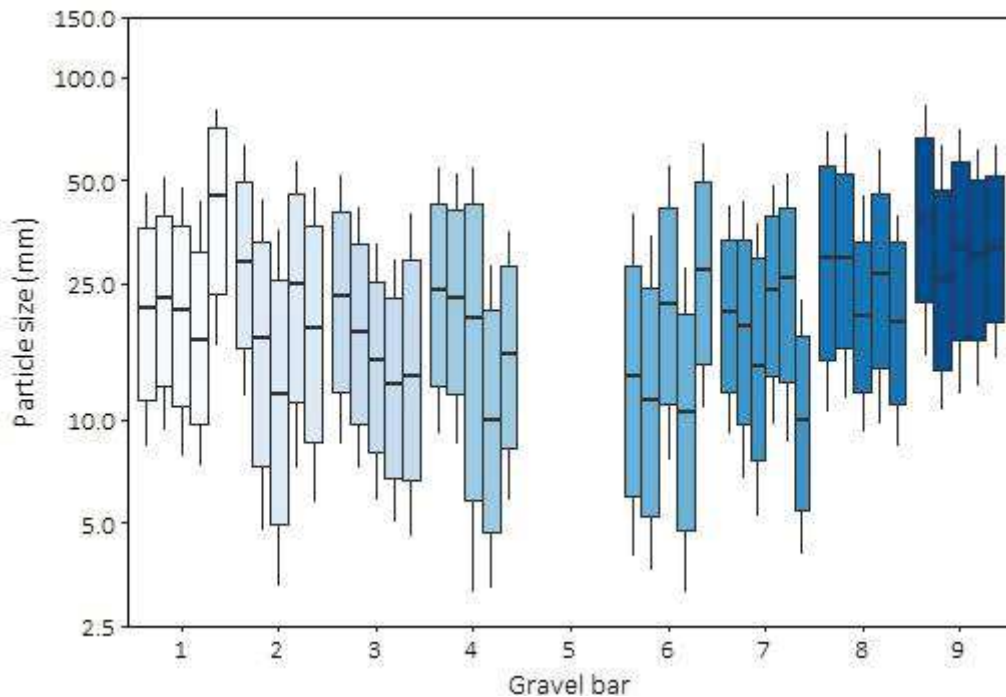


Figure 22. Boxplot representing the results from photosieving; tips of boxplots =  $D_{16}$  and  $D_{84}$ ; edges of boxplots =  $D_{25}$  and  $D_{75}$ ; centre =  $D_{50}$ . Each box represents a different patch photographed, with 5 photographs taken on each bar. See Figure 7. Schematic to show the spatial distribution of gravel bars (numbered 1 to 9) and data collected at each one to help characterise riverbed conditions. Figure 7 and Figure 21 for bar numbering.

Results from the boxplots (Figure 22) show similar trends to the Wolman pebble counts (Figure 21), with more details about fine sediments. Bars located at the very top (1) and bottom (8 and 9) of the study reach are made of coarse material, with no fine sediments ( $D_{16} > 7$  mm). Inversely, gravel bars found towards the middle of the section show very low  $D_{16}$ , illustrating the high proportion of sand and silt, with the  $D_{50}$  as low as 10 mm in places. While interesting, the main value of these GSD data is for hydraulic modelling (e.g. for roughness estimates) and a baseline against which future changes can be assessed.

### 3.4.1 Bed mobility

Information on bed mobility can be gathered from the analysis of painted patches. The sizes of displaced painted particles after a flood provide information about the competence of this event, while particles that did not move show the limits of the event to entrain particles.

A flood event (or maybe several) occurred between the two field visits (estimated from flood marks as lower than bankfull stage) and some changes were observed on some of the painted patches (Figure 23). These changes were of different nature and reveal the different dynamics at play in different parts of the river. Patches on two bars (bars 3 and 5) showed no clear signs of change (=stability), or at least no change that could be attributed to flow (i.e. there was evidence of just a very small number of small clasts being displaced, but this was so limited that it could have been the result of the action of invertebrates or birds). Several particles of the patch painted on bar 7 were displaced and some were recovered at distances between 0.1 and 25 m downstream. It is important to highlight that some may have moved further but were not found (e.g. displaced out of the bar and/or in the wetted channel). In addition, unpainted sediments were found on top of the patch, showing that particle movement was not limited to the patch itself but likely occurred over much of the bar.

Finally, no particle movement was observed on the bar 9, but the patch was densely covered with sand. Here although the flood event was of the same magnitude as the other locations, sediment dynamics were more depositional than erosional.

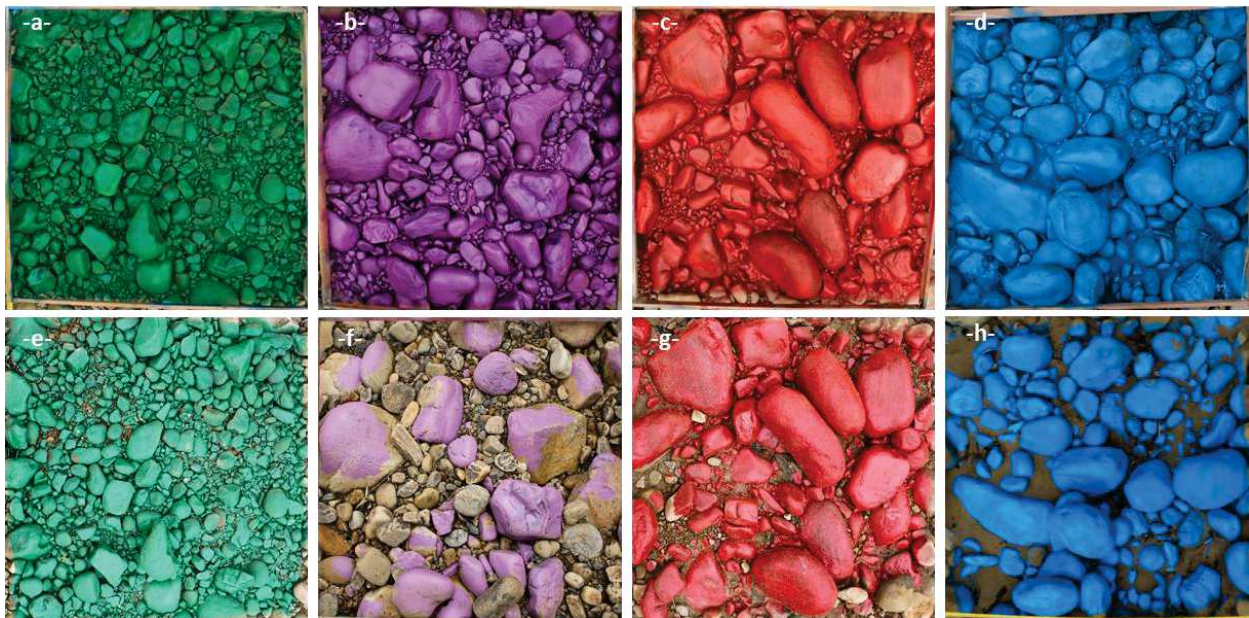


Figure 23. Illustration of the different processes observed from painted patches, located on different gravel bars of the River Trusan; bar 3 (-a- & -e-), bar 5 (-b- & -f-), bar 7 (-c- & -g-) and bar 9 (-d- & -h-).

### 3.4.2 Bed armouring

The image-based technique described in the methods section was applied on 3 gravel bars (see locations on Figure 3). This technique is not commonly used in the literature because it underestimates the median particle size of the subsurface material. Nevertheless, as it was not possible to manually quantify armouring (this would involve removing large volumes of material) the image-based approach was used estimate armouring ration for bars within the study section. An example illustrating the difference between surface and subsurface material at one of the sampling points is presented in Figure 24.

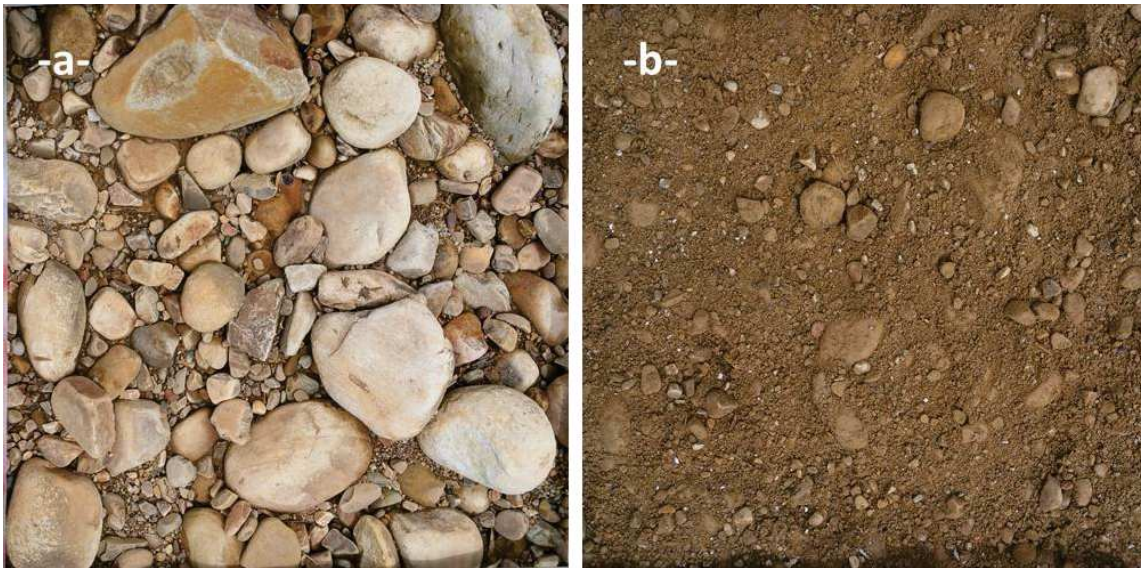


Figure 24. Example of the surface (-a-) and subsurface (-b-) particle size from the same patch.

It appears that the armouring ratio of gravel bars decreases downstream (Table 4). Using the traditional method, an armouring ratio of 3.6 would represent a very high armouring. Armouring occurs naturally in rivers, but can be exacerbated by human activities. In particular, it tends to increase when coarse sediment supply from the catchment is reduced, and/or when large volumes of fine sediment deposit within the gravel matrix. The higher armouring ratios of gravel bars upstream reflect the higher human interferences (bank stabilisation, landslides, cattle access to the river, etc.). Although bank erosion is very pronounced in the downstream part of the river, it seems that this geomorphic activity allows the river to rework its bars, thus limiting armouring.

Table 4. Armouring ratio estimated for 3 gravels bars following the method described in Part 1.

Gravel bar	Surface $D_{50}$ <i>mm</i>	Subsurface $D_{50}$ <i>mm</i>	Armouring ratio
2	10.40	2.90	3.59
5	9.60	3.90	2.46
9	12.80	6.93	1.85

### 3.5 Hydraulic modelling

Model calibration was undertaken for the discharge recorded on the days that we surveyed the hydraulic cross sections (see Section 2.3.2; i.e.  $5.97 \text{ m}^3 \text{ s}^{-1}$ ); this also corresponds to the discharge prevailing during the UAV-based survey. Water lines (and hence wetted width) observed on the aerial orthomosaics were used to help validate model outputs at this discharge. Because of our desire to understand factors influencing erosion, once calibrated, model simulations were made for bankfull stage. The value of discharge associated with the bankfull stage was estimated from the model outputs in locations where no severe bank erosion was observed (i.e. channel geometry close to natural); is defined as the discharge for which the entire wetted perimeter is underwater, but before water overtops the banks. On average, bankfull discharge was estimated at approximately  $75 \text{ m}^3 \text{ s}^{-1}$ . Shear stress is used to represent flow energy at this discharge, as it is the physical force (in  $\text{Newtons m}^{-2}$ ) applied to the river bed and banks.

The upper reach (Figure 25; Reach 1 in Figure 3) shows high shear stresses in places where depth is low to moderate as flows are turbulent. The entrance of the bend, where the right bank is clearly exposed (i.e. land cleared and high sediment delivery into the channel), shear stresses are also very high and so water hits the banks at high velocity and force. The energy is then rather well dissipated, with the section directly downstream from the bend being very deep and having low shear stresses (i.e. low velocities) and easily subject to deposition of finer particles (such as the ones eroded from the exposed bank upstream). This is supported by field observations of fine material accumulating on the surface of the bar in this area.

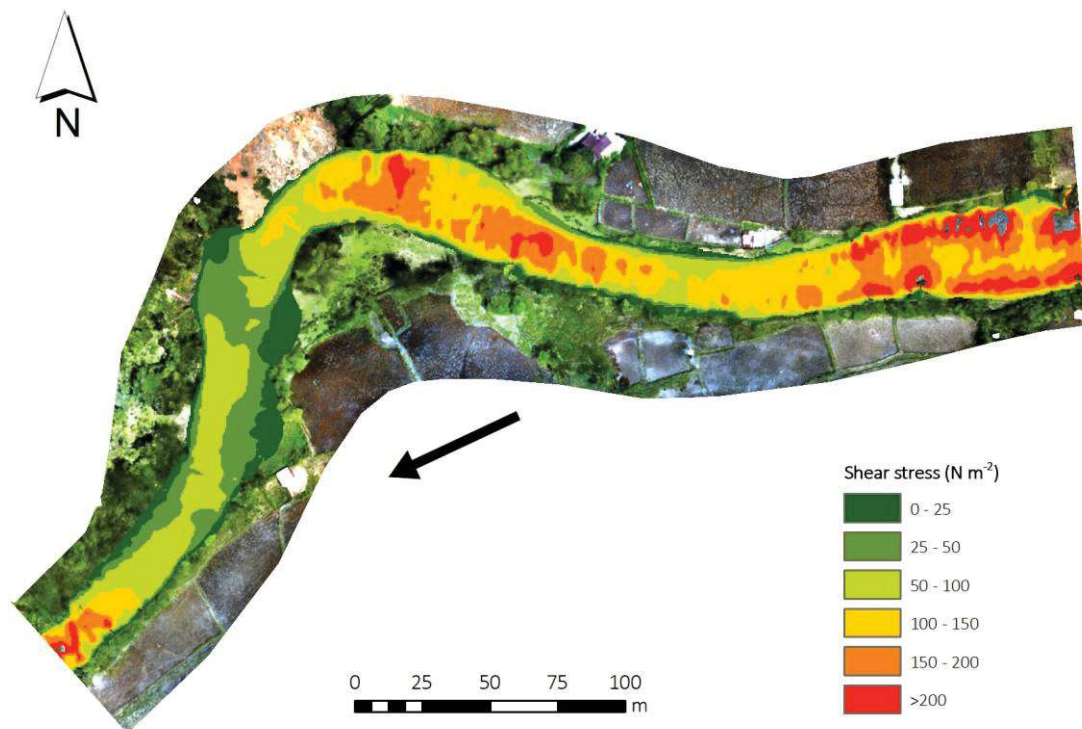


Figure 25. Shear stresses estimates from the 2D model at bankfull discharge ( $Q = 75 \text{ m}^3 \text{ s}^{-1}$ ) for the upper reach (Reach 1 in Figure 3).

The model output for the middle reach (Reach 4 in Figure 3) is shown in Figure 26. This reach was fully channelized upstream from the road bridge (located approximately in the middle of Figure 26, adjacent to the flow direction arrow). At bankfull, the channelized section is clearly homogeneous with high shear stresses ( $>100 \text{ N m}^{-2}$ ) over the entire width of the channel, initiating an accelerated area of flows concentrated under the bridge that generate very high shear stresses in the vicinity of the bridge as well as further downstream. As the water moves downstream, it appears that shear stresses are not particularly high on the outside the bend. Stresses are higher on the inside; this corresponds with field observation of rather intense erosion of exposed banks in these areas, despite them being outside the wetted channel at low flows.



Figure 26. Shear stresses estimates from the 2D model at bankfull discharge ( $Q = 75 \text{ m}^3 \text{ s}^{-1}$ ) for the middle reach.

The last reach modelled (section 6 in Figure 3) is presented in Figure 27. Although the discharge modelled is the same as Figure 25 and Figure 26, flows overtop the banks in most of the section. Clearly, what is a bankfull flow upstream is not bankfull here, so there is a change in channel geometry that makes bankfull flow slightly lower. This may mean that (i) sedimentation occurs in this section, changing the wetted area/Q relationship compared to upstream, (ii) flooding occurs where there is erosion and the water can enter to the floodplain through specific locations, or (iii) the 2 upstream sections are incised and their cross-sectional geometry is slightly different than the downstream one. The extensive gravel bars in this lowest section suggest that # (ii) may offer the best explanation.

Shear stresses are predicted to be particularly high at the bottom end of this reach. Generally, shear stresses are not particularly high in the section and, most interestingly, are not very high

in locations suffering from severe erosion (see arrows). This, along with the observations made earlier about the importance of the absence of vegetation, illustrates that hydraulics is not directly responsible for the occurrence of severe erosion along these banks. A combination of bank material properties (i.e. loose fluvial material) and the lack of trees rendered these areas sensitive to erosion even for the moderate shear stresses that occur during bankfull discharges.



Figure 27. Shear stresses estimates from the 2D model at bankfull discharge ( $Q = 75 \text{ m}^3 \text{ s}^{-1}$ ) for the lower reach.

Key points

1. There is no systematic downstream change in sediment grain sizes through the study section, although some bars are slightly coarser than others.
2. Bed stability, as indicated by the painted patches, also varies; in response to the same flow events, some locations were experiencing marked scour while in other locations the dominant process was sediment deposition.
3. Hydraulic models for bankfull discharge indicated that areas experiencing high shear forces are frequently those where erosion is evident. The model for the middle section indicated that channel engineering here leads to increased shear stresses immediately downstream, and may be contributing to erosion risk.
4. The hydraulic models also showed that erosion is occurring in some areas despite the fact that shear stresses remain only moderate at bankfull discharge. These areas are those where the riparian zone has been completely cleared and used for grazing, and buffalo are allowed direct access to the riverbanks.

## 4 Conclusions from the assessment of factors influencing erosion

1. There is no evidence of spatially extensive changes in land use in the Upper Trusan catchment in recent years. However, there is deforestation in some smaller sub-catchments, and this corresponds directly to adjacent downstream areas that have experienced overbanks flows and siltation of rice paddies.
2. There is no evidence of change in annual precipitation within the Trusan catchment over the last 50 years. Despite growing evidence of climate change all over the world, this cannot be argued as the main factor of hydrological changes reported in this catchment.
3. Of the 5.2 km section of river surveyed, 30% was considered as experiencing high or severe erosion, and another 28% mild erosion. Erosion consists of slab failure, undermining of banks (i.e. geomorphic processes) and erosion due directly to human activities, including cattle trampling.
4. There are three major landslides within the study section (all in the upper part), each delivering fine sediment to the river channel. Each of these areas is associated with (can be attributed to) localised clearance of the forest on the hillslope above.
5. Although the water buffalo themselves are not always visible, it is evident from field assessment of the conditions in the riparian zones and adjacent hillslopes that the cumulative impact of these animals on the morphology of the area is great; they are major agents of zoo-geomorphology. Their impact includes not just the direct collapse of localised sections of bank, but the formation of gullies and furrows on cleared areas of land, perpetually muddy tracks etc.
6. Multivariate analysis indicated that areas of severe and high erosion are statistically associated with the clearance of riparian vegetation. On the other hand, areas suffering no or only mild erosion were characterised by dense riparian cover and/or large gravel bars that protect the banks.
7. Hydraulic models provided important insights that support some of the conclusions drawn from previous aspects of the work. Models were run for bankfull stage, as at this discharge hydraulic forces are generally at their maximum. A particularly important conclusion from the models was that not all places experiencing erosion have high shear stresses during bankfull flow; places experiencing some of the worst erosion have only moderate shear stress, and these are areas completely devoid of their natural riparian vegetation.

8. Although there are some clear patterns and cause-effect relations are self-evident in some places, some things observed in the field remain less clear. For example, some areas without any erosion were close to places where erosion was severe. Differences may be related to factors not assessed in this study, notably the cohesiveness and water content (degree of saturation) of bank materials. They could also be to do with differences in localised slope, sediment grain sizes (larger sediments preventing scour) or river bend curvature. Quite possibly several of these factors are acting together to influence the likelihood of erosion in the Trusan. As discussed in the accompanying report (Marteau et al., 2008), river erosion is a natural phenomenon that should be expected, especially in high energy systems such the Trusan. Rivers can and do change their course naturally, and so it is possible that some of the erosion observed is not directly attributable to human causes (i.e. it is within natural bounds; see discussion in Marteau et al., 2018).
9. The temporal coverage and quality of the hydrological data available for the River Trusan are inadequate for the purpose of assessing whether flood frequency or magnitude are increasing. This is unfortunate but it is how it is. Nevertheless, based on the accumulated knowledge of hydrological studies worldwide, it is possible to argue with confidence that if catchment and riparian areas continue to be cleared of trees, flooding and erosion issues will intensify.
10. Effects of catchment scale changes often require of some time to be detected downstream. It is clear that the Upper Trusan catchment has suffered changes in structural connectivity to some degree (e.g. related to patchy forest clearance, access tracks) and it is possible that the full effects of these past changes have not yet been felt in the river channel. This stresses the need for ongoing monitoring, both to determine lag effects and help with assessment of the success of implemented to help deal with erosion and flooding issues.

## 5 Recommendations

We frame discussion of recommendations for the River Trusan around the three management scales outlined in the *Review of Best Practice* document written by *Marteau et al.* (Marteau *et al.*, 2018).

### 5.1 Catchment scale

There should be a concerted and co-ordinated effort to limit deforestation in the catchment upstream of and within the study section. This may not be easy, nor may it be something which can be accomplished immediately, but it should be a long-term goal of the sustainable management initiative currently underway in the Upper Trusan. It will involve liaison between local communities, government agencies and logging companies. WWF have been centrally involved in a number of activities in the Trusan, including funding the current work, and it is logical to include them in future river management initiatives.

Detailed assessment of who has been or is currently responsible for forest clearance is beyond the scope of the present study, but it is clear that several actors are involved, although the nature, magnitude and spatial distribution of their contribution to catchment-scale changes most likely differs.

Tracks act as conduits for both water and fine sediment and can have a marked influence on river responses to rainfall. Major episodes of access track construction were evident from the Landsat image analysis, but evidence from recent images suggests that few new tracks have been built in the last 10-12 years. One focus of catchment-scale work should be to try to maintain this situation; thus, as far as possible, a policy of no or extremely few new tracks should be implemented. If new tracks are considered essential, they should be built and maintained in ways that limit their effect on runoff. Guidelines for this can be found in *Croke et al.* (1999) *Shaver & Clode* (2009). Monitoring of any new tracks should be put in place to allow assessment of how they impact runoff of water and fine sediment. Such monitoring can serve as a means of initiating remedial action (if necessary) and as demonstration of how tracks can impact hydrological processes and fine sediment loads entering tropical rivers.

Several problematic tracks and access routes were encountered during field surveys. The most severe of these, particularly in terms of contributing to fine sediment entering the river, are pictured in Plate 2 and 3. Options for installing bunds or silt traps in these two locations should be considered as part of a wider catchment-scale strategy to address issues raised by access tracks. A related problem is that access tracks frequently cross tributaries that drain into the Trusan. Many crossing points are fords, which can contribute to destabilisation of bed and bank conditions in the tributaries and further release fine sediments. Where possible, in

locations where tracks cross tributaries, bridges should be considered as a means of limiting the collateral impacts of access.

Analysis of Landsat images indicated that forest still covers 95% of the Upper Trusan catchment. Some clearance was evident between 2007 and 2014, but the most intense clearance occurred between 2014 and 17. This was very localised (confined to the Sg. Rengir sub-catchment) and, based on discussion with local communities, is clearance for timber. We recommend that relevant authorities enter into discussions to try to curtail future clearance of this kind. While not spatially extensive, this clearance has contributed to the flooding and siltation of rice paddies in the area immediately downstream so is directly impacting the local communities. Other localised clearances provide further evidence of the impacts of forest loss – the three main landslides detailed in Section 3.3 (also see Plate 4) can all be attributed to local clearance of forest on the steep slopes above the river channel. Again, there needs to be a dialogue with local people to try to prevent such clearance, however localised, and especially where it is close to the river channel.



*Plate 2. Bridge at Punan Trusan. These images show water entering the river from an access track (left), and how the plume of fine sediment is conveyed downstream, resulting in a visible increase in turbidity across the channel. March 2018.*



*Plate 3. Track on hillslope approximately 1 km above Punan Trusan. This image was taken during a late afternoon thunderstorm. March 2018.*



*Plate 4. An example of a major landslide associated with localised forest clearance.*

Additionally, we recommend an evaluation of the potential impacts on sediment connectivity before any intervention at the catchment is executed. Cavalli *et al.* (2013) developed an Index of Connectivity (IC), which is based upon the original approach by Borselli *et al.* (2008), that allows mapping (raster-based) and quantitative assessment of the spatial distribution of structural connectivity. The inputs needed by this Index are (a) terrain data (extracted from the DEM) and (b) land use maps (extracted from satellite images). Therefore, the degree to which hill-slopes are connected to channels can be mapped. The inputs for the Index can be modified according to different scenarios, based on the planned intervention(s). Once modified, a new map of connectivity can be calculated and compared to what is termed the actual situation or condition. The comparison of maps can be used as tool to identify potential risks associated to the increase and decrease of sediment connectivity. Although the maps of

connectivity do not provide quantitative estimates of sediment fluxes, they provide insights into how water and sediments are moving between the different compartments of the catchment. This approach therefore helps refine understanding of the hydrology and sediment dynamics (the likely fine sediment loads) of the channel. Connectivity analysis can be done as part of desk-top studies undertaken in parallel with field monitoring and instrumentation, and can be seen as a way to help interpret data collected and any future changes observed. If university-based researchers are involved in the monitoring and assessment (see 5.4. below), the connectivity analysis can be undertaken as part of their work.

## 5.2 River corridor scale

We propose adopting some aspects of the “erodible river corridor concept”, developed by several authors in the 1990s and presented in the Review of good practices associated with this report. This involves four interconnected proposals designed to help avoid future problems over extensive sections of the river.

First, we suggest some managed retreat from the riverbank zone in selected areas. The idea is to leave room for the river to erode and dissipate its energy in places where geomorphic activity is possible and risks are low (i.e. no population, no valuable land etc.). Three main areas are suggested to be left for the river (see Figure 28). Both the left and right banks of the river upstream from the road-bridge leading to Long Telingan can be left unprotected as this would help dissipate energy before the water reaches the bridge (i.e. natural protection from bridge undermining). The third area is located further downstream at the confluence of a small tributary. This stretch is situated between two sections with relatively high stability (strong riparian cover that protect the banks from erosion). The protection of these two sections is key as large rice paddies can be found on either side of the river. Leaving room for the river between these two critical sections can prevent any damage in the future (i.e. progressive or regressive erosion).

Second, we strongly recommend some sort of community-wide agreement on stopping any further clearance of riparian vegetation. This clearly requires careful and sensitive dialogue between various stakeholders, but in combination with some localised measures to prevent further erosion in areas already cleared (for which see Section 5.3), this is one of the most significant steps that could be taken to help prevent erosion. Very often the clearance of riparian areas can be attributed directly or indirectly to rice growing – either expanding paddies as close to the riverbank as possible, or else expanding pasture areas where buffalo used seasonally in the paddies are allowed to graze (Plate 5).

The third proposal involves better management of the buffalo. At present they are used for a short period of the year, following harvest, to help prepare the ground within the paddy areas. Once this is over, they are left to roam freely. Cumulatively over time, this has had a major impact on the river corridor. At the very least, fences should be erected to confine buffalo to

less sensitive areas, and especially stop them entering the channel. In turn this requires drinking baths being placed and wallow holes being dug in certain areas, to ensure buffalo have access to water and other key needs. Fences to stop them entering the channel can also help demarcate the riparian zone, and then used to increase the success of some of the more localised measures described below.

Fourth, and finally, we strongly recommend preventing any direct alteration of channel geometry in the vicinity of areas suffering from high and severe erosion. Bank stabilisation by moving boulders from the channel will only displace (and potentially worsen) the problem elsewhere by disturbing the natural equilibrium (although it should be seen as a 'dynamic equilibrium) of the river. There are one or two instances where boulders placed along banks have resulted in erosion behind them, such they are now sitting in the middle of the channel. If access is possible, such boulders could be removed to avoid any further erosion and displacement of high flow forces. One clear example of the unanticipated consequences of badly conceived intervention is the generation of high velocity areas under the bridge (as modelled at bankfull discharge); this may have direct and rapid consequences when it comes to stability of the bridge. Similarly, extracting gravel from the bed will have significant consequences on channel equilibrium.

Badly conceived interventions can have immediate effects on the stability of riverbanks and can quickly undermine months or years of bio-engineering efforts to maintain riverbank stability. It is important to ensure that the efforts undertaken by local communities are not ruined within days by the unawareness and inappropriate actions of others.

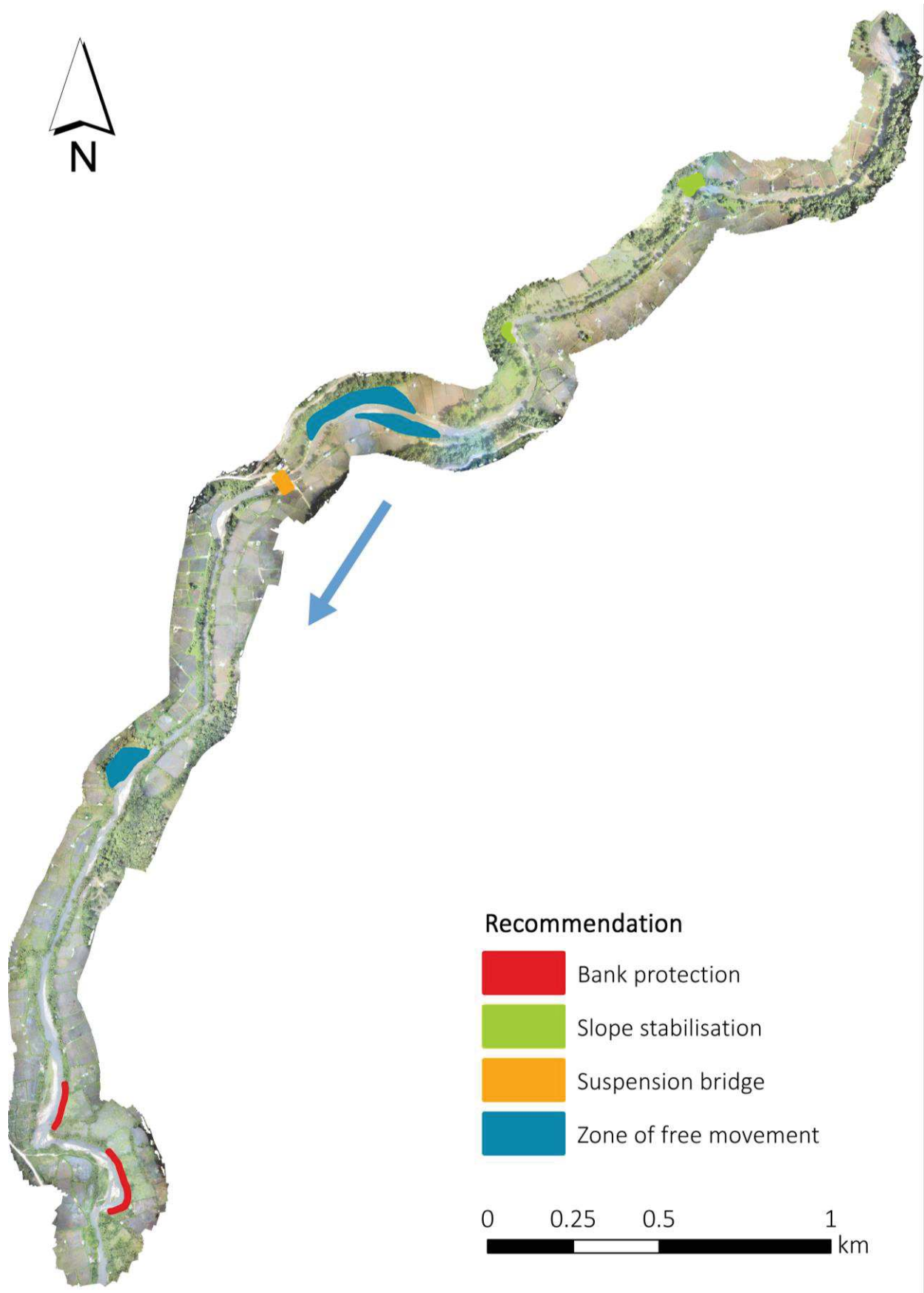


Figure 28. Map of recommendations proposed at the corridor scale for the Upper Trusan River.



*Plate 5. Example of a cleared riparian area, with pasture land extending all the way to the riverbank. Not only are the banks unprotected (i.e. no binding tree roots), but they have the additional pressure of being trampled by buffalo. The bank is undermined over a distance of approximately 100 m, with retreat in this area estimated from aerial images to have been in the order of 18 m in the last three years (March 2018).*

### 5.3 Localised interventions

There is a small number of places where local intervention may be needed to avoid further deterioration of channel conditions. ‘Soft’ or ‘bio-engineering’ approaches should be adopted – these are less expensive than traditional or hard engineering solutions and offer greater prospects for long term success. To aid discussion of these, Figure 17 is repeated below. The key point to stress is that these interventions should be implemented alongside the catchment and corridor scale management outlined above.

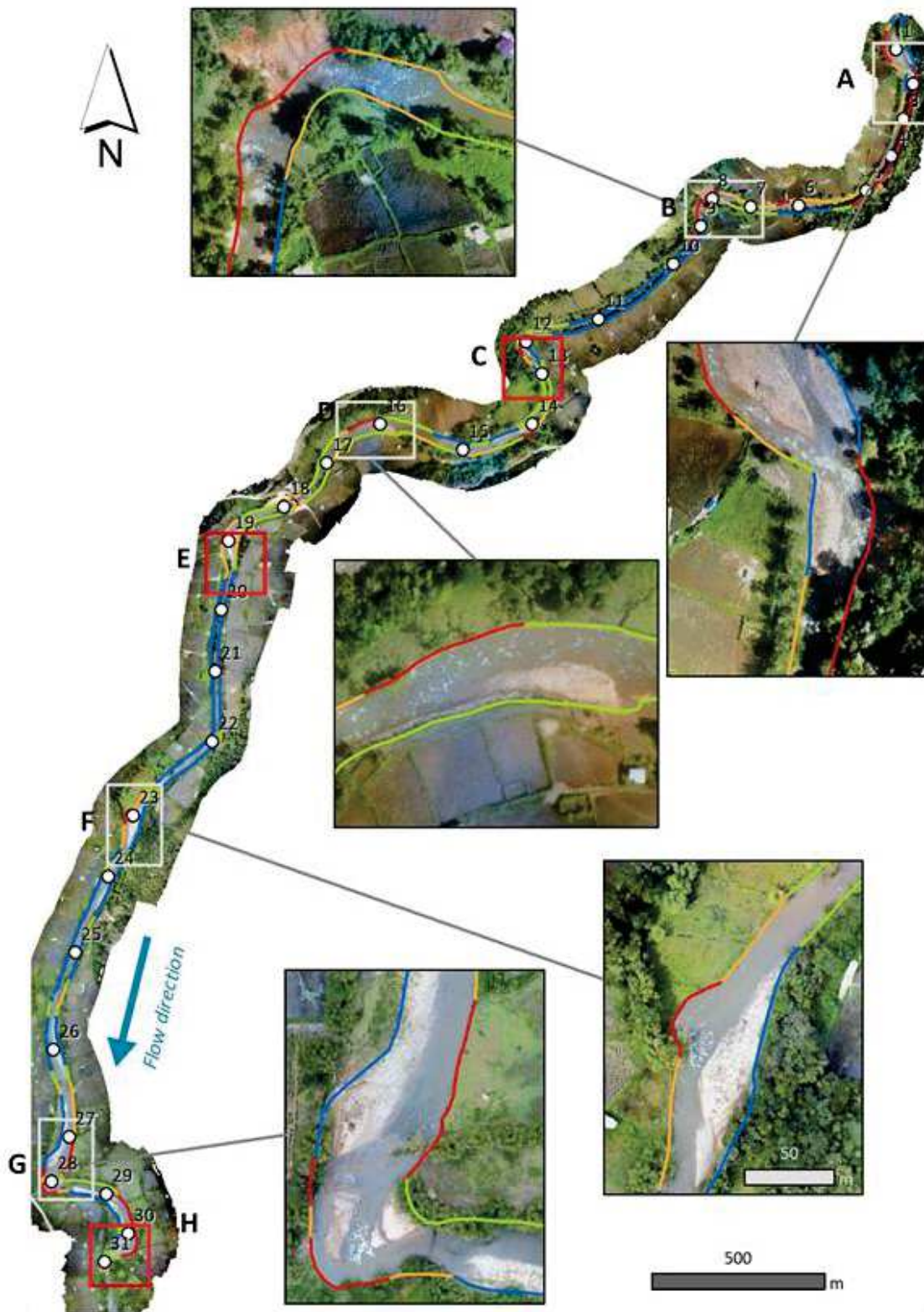


Figure 29. Map of erosion within the study section. Areas where localised measured may be considered are labelled A-F.

1. There are three major landslides within the study section (boxes A, B and C of Figure 29). Consideration should be given to covering these with geotextile matting to prevent further collapse and limiting runoff of fine sediment; they should be seeded with a fast-growing grass species to add further stability. Discussions should be had with local people to identify a suitable native species. If not, then Vetiver can be considered. This has been used successfully

in many countries in Southeast Asia (Marteau *et al.*, 2018). It may also be advisable (if slopes are not too great) to plant some live palisades along contours of these slopes (Marteau *et al.*, 2018). These are interim measures, designed to add stability to currently bare and unstable slopes until larger shrubs can colonise and grow to the point that they help bind the soil. This proposal is analogous to the work often carried out on the steep slopes of highway cuttings. Fences should be erected along planted areas to keep cattle out while grasses are taking hold. In parallel with this, the base of each area may need to be secured, depending on accessibility to the channel for the machinery required for this. So-called root wads can be used for this (Figure 30).

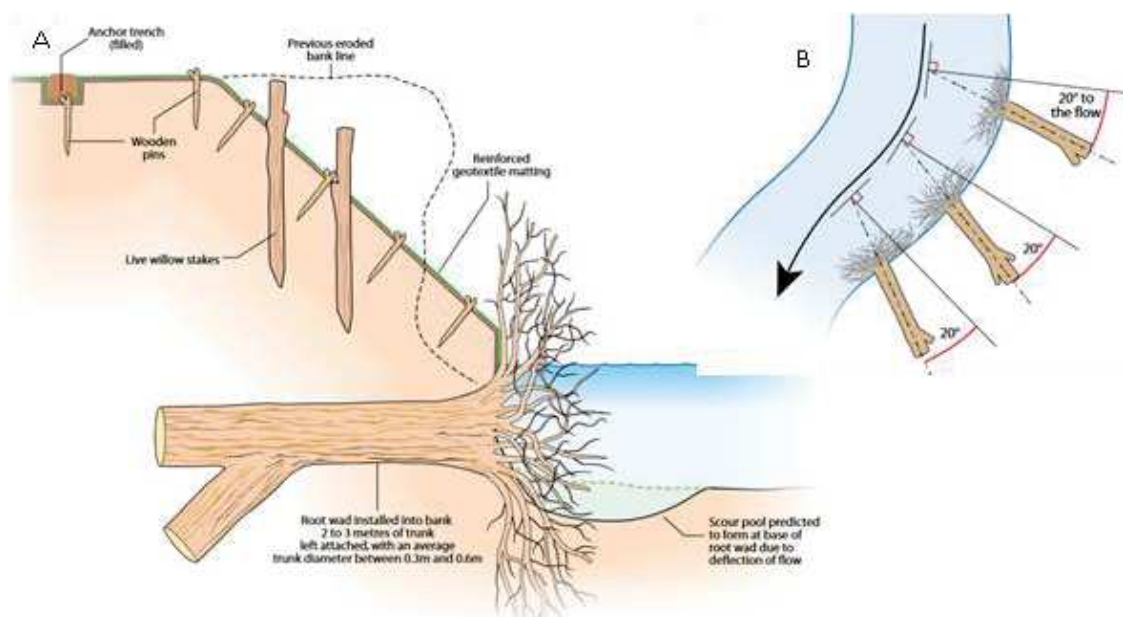


Figure 30. Root wads inserted into the base of a steep slope to prevent toe of the slope being eroded.

2. Area D in Figure 29 is proposed to be the subject of some corridor-scale management (as per Section 5.2). This section is where hard engineering measures have been implemented within the last year (channelization) to help prevent erosion. However, one potentially significant issue is that this channelization is resulting in high shear stresses downstream, and may contribute to further undermining of the road bridge. We suggest that rather than confining it, the river should be allowed to erode upstream, a process that will help dissipate the energy. Nevertheless, periodic floods may erode bridge supports. Bearing in mind the possibility that forest clearance upstream from here may result in an increased frequency and magnitude of floods, consideration should be given to changing to a suspension type bridge. This may not be immediate, but at the next time that bridge renovation works are deemed necessary.

3. At the downstream end of the study section, there are two areas of severe bank erosion (G and H in Figure 29; see Plate 5 Plate 6). Bank heights here are approximately 2-3 m. There are several options. One would be to insert root wads, using trees whose roots extend to bank

tops once inserted (Figure 31Figure 32). Alternatively, a fence made from the woody stems of a local plant (e.g. bamboo) could be built at the base of the slopes, providing short term protection. The area behind this can be filled with soil and bankside material (Figure 32), and seeded with local grasses or Vetiver, and planted with saplings for longer term stability. In parallel with whichever of these is adopted, cattle fences should be erected well back from the bank top and the riparian zone left to be colonised by trees and shrubs. Ideally to help this process, some planting of the riparian zone could be encouraged.



Plate 6. Erosion in the most downstream part of the study section (March 2018).

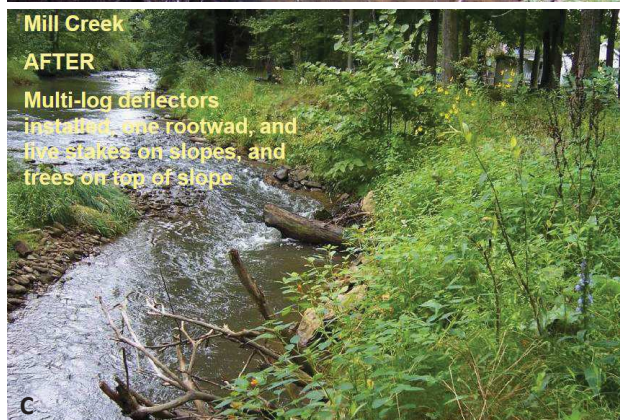
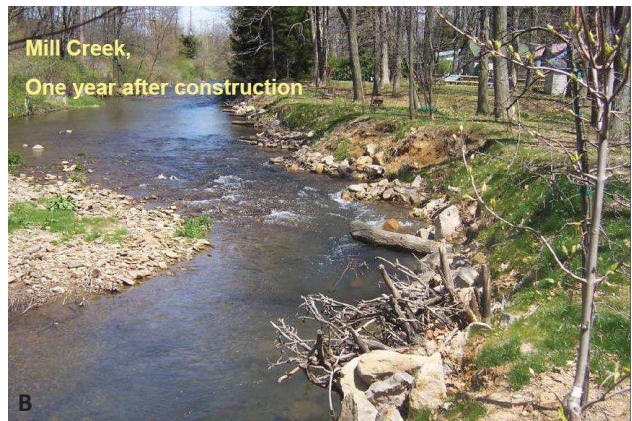


Figure 31. Photos of a fast-flowing river bend where a combination of root wads, log deflectors and live stakes were used for bank stabilisation. (Source: Rob Cronauer, Westmoreland Conservation District, 2016).

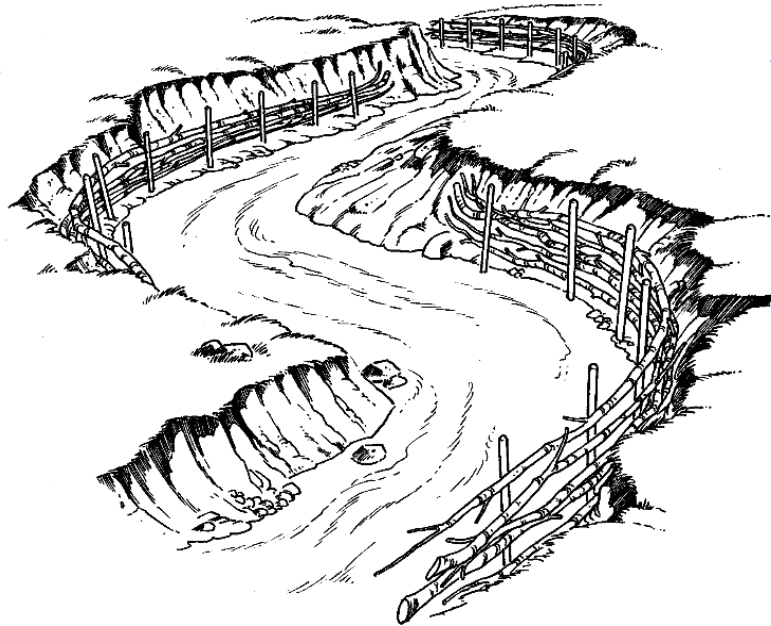


Figure 32. Live bank protection, used to control erosion of outside curves. Note that for clarity the backfill has been removed (Source: Polster, 2008).

## 5.4 The need for ongoing hydrological monitoring and survey

The work presented in this report represents a first attempt at understanding the causes of bank erosion and changes in the sedimentary activity of the Upper Trusan River, stemming from concerns voiced by riverside communities. Conclusions are based on a combination of long-term rainfall data, Landsat imagery, field-based assessment of geomorphological conditions and riverbank instability, and hydraulic modelling. However, the data available to us, limited duration and remit of the study meant that several potentially important factors have not been assessed - the role of tributaries, the importance of bank material properties, and long-term changes in hydrology in particular. Thus, we stress that conclusions of the current work should be considered as the first stage in understanding the function of the Upper Trusan as a hydrological system. Better understanding requires ongoing surveys and monitoring in a number of key areas. These can be summarised as:

- (i) Repeating the work undertaken for the present study; i.e. analysis of landcover change, and geomorphic surveys (ground and aerial) to map erosion and other geomorphic change. Such surveys should be conducted annually for the first 2-3 years following any localised intervention, then every 3-5 years thereafter.
- (ii) Monitor flow discharge at representative locations along the 5.2 km section.
- (iii) Instrument critical locations (downstream from major tributaries and landslides) to monitor turbidity continuously. From such data, fine sediment loads and budgets can be developed. It is unlikely that DID could be expected to instrument sites to

the degree necessary, so a more appropriate approach would be to involve university researchers/academics. This applies also to points iv and v.

- (iv) Monitor fine sediment delivery from tracks and roads, to start to quantify their contribution to river sediment loads.
- (v) Monitor the success of localised interventions, and revise/redesign accordingly.

## 6 Reference list

- Asner GP. 2009. Automated mapping of tropical deforestation and forest degradation: CLASlite. *Journal of Applied Remote Sensing* 3(1): 335-43.
- Borselli L, Cassi P, Torri D. 2008. Prolegomena to sediment and flow connectivity in the landscape: A GIS and field numerical assessment. *Catena* 75(3): 268–277.
- Bryan JE, Shearman PL, Asner GP, Knapp DE, Aoro G, Lokes B. 2013. Extreme Differences in Forest Degradation in Borneo: Comparing Practices in Sarawak, Sabah, and Brunei. *PLoS ONE* 8(7)
- Buscombe D. 2013. Transferable wavelet method for grain-size distribution from images of sediment surfaces and thin sections, and other natural granular patterns. *Sedimentology* 60(7): 1709–1732.
- Cavalli M, Trevisani S, Comiti F, Marchi L. 2013. Geomorphometric assessment of spatial sediment connectivity in small Alpine catchments. *Geomorphology* 188: 31–41.
- Croke J, Wallbrink P, Fogarty P, McCormack B, Hairsine P, Mockler S, Brophy J. 1999. Managing Sediment Sources and Movement in Forests: The Forest Industry and Water Quality. Cooperative Research Centre for Catchment Hydrology
- Gao BC. 1996. NDWI - A normalized difference water index for remote sensing of vegetation liquid water from space. *Remote Sensing of Environment* 58(3): 257–266.
- García-Ruiz JM, Arnáez J, Beguería S, Seeger M, Martí-Bono C, Regüés D, Lana-Renault N, White S. 2005. Runoff generation in an intensively disturbed, abandoned farmland catchment, Central Spanish Pyrenees. *Catena* 59(1): 79–92.
- Marteau B, Gibbins C, Batalla RJ, Vericat D. 2018. Review of good practice in managing riverbank instability and erosion - A WWF-Malaysia Report
- Marteau B, Vericat D, Gibbins C, Batalla RJ, Green DR. 2016. Application of Structure-from-Motion photogrammetry to river restoration. *Earth Surface Processes and Landforms* 42: 503–515.
- Petts GE, Gurnell AM. 2005. Dams and geomorphology: Research progress and future directions. *Geomorphology* 71(1–2): 27–47.
- Shaver E, Clode G. 2009. Forestry Erosion & Sediment Control - Hawke's Bay Waterway Guidelines. Hawke's Bay Regional Council: 74 pp.
- US Army Corps of Engineers. 2018. HEC-RAS Version 5.0.4
- Westoby MJ, Brasington J, Glasser NF, Hambrey MJ, Reynolds JM. 2012. "Structure-from-Motion" photogrammetry: A low-cost, effective tool for geoscience applications. *Geomorphology* 179: 300–314.
- Wolman MG. 1954. A method of sampling coarse river-bed material. *Transactions, American Geophysical Union* 35(6): 951–956.

## 7 Appendices

Appendix Km0.



Appendix Km0.1.



Appendix Km0.1 (continued).



Appendix Km0.2.



Appendix Km0.3.



Appendix Km0.3 (continued).



Appendix Km0.4.



Appendix Km0.4 (continued).



Appendix Km0.4 (continued).



Appendix Km0.6.



Appendix Km0.6 (continued).



Appendix Km0.8.



Appendix Km0.8 (continued).



Appendix Km0.8 (continued).



Appendix Km0.9.



Appendix Km0.9 (continued).



Appendix Km1.0.



Appendix Km1.0 (continued).



Appendix Km1.1.



Appendix Km1.1 (continued).



Appendix Km1.4.



Appendix Km1.4 (continued).



Appendix Km1.4 (continued).



Appendix Km1.6.



Appendix Km1.6 (continued).



Appendix Km1.6 (continued).



Appendix Km1.7.



Appendix Km1.8.



Appendix Km1.8 (continued).



Appendix Km2.0.



Appendix Km2.0 (continued).



Appendix Km2.3.



Appendix Km2.3 (continued).



Appendix Km2.5.



Appendix Km2.5 (continued).



Appendix Km2.7.



Appendix Km2.7 (continued).



Appendix Km2.8.



Appendix Km2.8 (continued).



Appendix Km3.0.



Appendix Km3.0 (continued).



Appendix Km3.0 (continued).



Appendix Km3.2.



Appendix Km3.2 (continued).



Appendix Km3.2 (continued).



Appendix Km3.4.



Appendix Km3.7.



Appendix Km3.7 (continued).



Appendix Km3.9.



Appendix Km4.1.



Appendix Km4.4.



Appendix Km4.4 (continued).



Appendix Km4.7.



Appendix Km4.7 (continued).



Appendix Km4.8.



Appendix Km4.8 (continued).



Appendix Km5.0.



Appendix Km5.0 (continued).



Appendix Km5.1.



Appendix Km5.1 (continued).



### **About WWF-Malaysia**

WWF-Malaysia (World Wide Fund for Nature-Malaysia) was established in Malaysia in 1972. It currently runs more than 90 projects, covering a diverse range of environmental conservation and protection work, from saving endangered species such as tigers and turtles, to protecting our highland forests, rivers and seas. The national conservation organisation also undertakes environmental education and advocacy work to achieve its conservation goals. Its mission is to stop the degradation of the earth's natural environment and to build a future in which humans live in harmony with nature, by conserving the nation's biological diversity, ensuring that the use of renewable natural resources is sustainable, and promoting the reduction of pollution and wasteful consumption.

### **WWF-Malaysia**

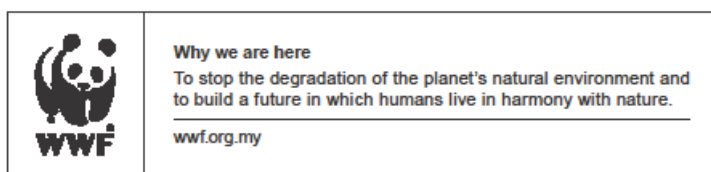
1 Jalan PJS 5/28A  
Petaling Jaya Commercial Centre (PJCC)  
46150 Petaling Jaya  
Selangor, Malaysia

Telephone No: +603 7450 3773

Fascimile No: +603 7450 3777

Email: [contactus@wwf.org.my](mailto:contactus@wwf.org.my)

**[wwf.org.my](http://wwf.org.my)**



© 1986 panda symbol WWF – World Wide Fund for Nature (Formerly World Wildlife Fund)

® “WWF” is a WWF registered trademark